Journal of Sound and Vibration (2002) **257**(1), 19–62
doi:10.1006/jsvi.5026, available online at http://www.idealibrary.com on IDEAL®

IMPROVEMENT OF THE SEMI-ANALYTICAL METHOD, FOR DETERMINING THE GEOMETRICALLY NON-LINEAR RESPONSE OF THIN STRAIGHT STRUCTURES: PART II—FIRST AND SECOND NON-LINEAR MODE SHAPES OF FULLY CLAMPED RECTANGULAR PLATES

M. El Kadiri and R. Benamar

Laboratoire d'Etudes et de Recherches en Simulation, Instrumentation et Mesures, LERSIM, E.G.T. E.M.I., Université Mohamed V, BP 765 *Agdal Avenue Ibn Sina, Rabat, Morocco.*
E-mail: rbenamar@emi.ac.ma

(*Received* 29 *May* 2001, *and in final form* 4 *December* 2001)

In a previous series of papers, a semi-analytical model based on Hamilton's principle and spectral analysis has been developed for geometrically non-linear free vibrations occurring at large displacement amplitudes of clamped–clamped beams and fully clamped rectangular homogeneous and composite plates. In Part I of this series of papers, concerned with geometrically non-linear free and forced vibrations of various beams, a practical simple "multi-mode theory", based on the linearization of the non-linear algebraic equations, written in the modal basis, in the neighbourhood of each resonance has been developed. Simple explicit formulae, ready and easy to use for analytical or engineering purposes have been derived, which allows direct calculation of the basic function contributions to the first three non-linear mode shapes of the beams considered. Also, various possible truncations of the series expansion defining the first non-linear mode shape have been considered and compared with the complete solution, which showed that an increasing number of basic functions has to be used, corresponding to increasingly sized intervals of vibration amplitudes; starting from use of only one function, i.e., the first linear mode shape, corresponding to very small amplitudes, for which the linear theory is still valid, and ending by the complete series, involving six functions, corresponding to maximum vibration amplitudes at the beam middle point up to once the beam thickness. For higher amplitudes, a complementary second formulation has been developed, leading to reproduction of the known results via the solution of reduced linear systems of five equations and five unknowns. The purpose of this paper is to extend and adapt the approach described above to the geometrically non-linear free vibration of fully clamped rectangular plates in order to allow direct and easy calculation of the first, second and higher non-linear fully clamped rectangular plate mode shapes, with their associated non-linear frequencies and non-linear bending stress patterns. Also, numerical results corresponding to the first and second non-linear modes shapes of fully clamped rectangular plates with an aspect ratio $\alpha = 0{\cdot}6$ are presented. Data concerning the higher non-linear modes, the aspect ratio effect, and the forced vibration case will be presented later.

1. INTRODUCTION

New materials with high stiffness-to-weight ratio, such as those made of fibre-reinforced plastics, are becoming increasingly used to build high-performance structures which are

0022-460X/02/$35.00

required for aerospace applications. Also, to reach the performance required in the latest applications, even when classical isotropic materials are used, the necessary weight saving cannot be achieved unless the structures are designed with the lowest possible thickness. In both cases, if resonant behaviour occurs, the amplitude of the dynamic response will be relatively high and fatigue may occur [1, 2]. The geometrical non-linearity due to the high displacement amplitudes occurring in severe environment or in the neighbourhood of resonances has to be properly taken into account in the design of the structural components considered. Non-linear analysis methods are therefore necessary to predict the non-linear structural behaviour at large vibration amplitudes, and establish the appropriate design criteria [3, 4].

In spite of the considerable research which has been carried out in the last few decades, concerned with plate vibrations [5], no exact solution for the complicated problem of non-linear vibrations of rectangular plates is known. Even in the linear case, approximate numerical methods, like finite difference techniques, the Galerkin technique, Weinstein's method, integral equations and series methods have been used in the literature to determine the linear mode shapes and natural frequencies of fully clamped rectangular plates (FCRP) [6]. The only case of a rectangular plate for which exact linear analytical results are available is that of a plate with two opposite edges simply supported. A comprehensive treatment of the linear problem and references corresponding to all of the above-mentioned methods are given in the monograph of Leissa [7], and in his more recent review [8]. The non-linear analysis of plates has been for many years a subject of high interest and has led to the publication of reference books [9, 10]. Also, although a large number of studies have been carried out on non-linear plate vibrations, each problem has received a special treatment involving some particular approximations. Some of the relatively older models available, such as those proposed in references [11, 12], are based on the perturbation procedure, and, consequently, are practically limited to the first order effects of finite displacements upon natural frequency, as has been mentioned in reference [13]. Also, in most of the studies carried out on non-linear vibrations of rectangular plates, the common approach to such problems had been to assume a spatial function, usually the linear mode shape, and seek a solution for the time variable, assuming that the space and time functions can be separated, which is an assumption which does not rigorously hold in the non-linear case, as has been noticed in the early paper of Chu [14]. More recently, the hierarchical finite element method, denoted in what follows as the HFEM, has been proposed to study the first and higher non-linear modes of vibrations of FCRP, using the von Karman type of geometrical non-linear strain–displacement relationships, and the harmonic balance method, to derive the equations of motion [15, 16]. This approach has also been used in reference [17] to solve the equations of motion by the Newton and continuation methods and applied to the study of the non-linear free and steady state periodic forced response of plates, both homogeneous and composite. Another approach [18], called the asymptotic numerical method, has been developed for large-amplitude free vibrations of thin elastic plates. It is based on a combination of the perturbation method and the finite element method, and it eliminates the limitation of the validity of the classical perturbation method, practically restricted to weak non-linearity [13].

On the other hand, it may be noted that, as stated in reference [19], in spite of the considerable amount of research which has been carried out in the last few decades on non-linear vibrations, linear theories remain widely used in most of the practical applications, particularly in the field of modal testing. This may be attributed, as stated in reference [20], among other reasons, to the fact that the various attempts to describe mathematically the non-linear structural dynamic behaviour which have been developed and presented in the literature still appear somewhat esoteric and difficult to deal with in

practical situations. Also, no equivalence has been found, in the non-linear case, to the powerful and nice description of the linear dynamic behaviour of a structure, in terms of its natural frequencies and natural modes of vibration. The various attempts made in the last two decades by Benamar and co-workers, reported in references [6, 13, 19, 21–27], to describe the non-linear behaviour of some structures with a relatively simple geometry, such as beams, plates, and circular cylindrical shells, using their normal mode bases, show that although the development of such an equivalence may be a laborious task, the concept of normal modes of vibration remains in the non-linear case very useful and yields a deep insight into the structural dynamic behaviour. This has been shown theoretically by the considerable computing time saving and the relative mathematical simplicity of the non-linear semi-analytical models developed, in which linear mode shape bases are used to expand the unknown displacement series. Also, experimental measurements of an FCRP non-linear response harmonic distortion spatial distribution have been carried out in reference [24]. It was shown that this distribution was related to the plate linear mode shapes. Therefore, it was thought that investigations could be directed toward a further step in the development of a sort of "non-linear modal analysis theory", allowing direct determination of the non-linear mode shapes, the non-linear frequencies, and the associated non-linear bending stress patterns of thin straight structures, for the vibration amplitude ranges of interest in practical applications. It was also hoped that such an attempt could provide users with simple formulae, ready to use for analytical and engineering purposes, which would be much more practical than the published tables of data, obtained from the numerical iterative solution of a non-linear algebraic system, which necessitates the use of appropriate software in each case. Part I of this series of papers [20] was concerned with beams, with the objective of developing a practical simple "multi-mode theory", based on the linearization of the non-linear algebraic equations, written on the modal basis, in the neighbourhood of each resonance.

The purpose of this paper is the extension of this approach to geometrically non-linear free vibration of FCRP in order to allow direct calculation of the first, second, and higher non-linear FCRP mode shapes, with their associated non-linear frequencies and bending stress patterns. In section 2, a review of the theory and some numerical results obtained by solving iteratively the non-linear algebraic equations, for the first and the second non-linear mode shapes of FCRP, published previously, are summarized. Section 3 is concerned with the development of the new approach for free vibration analysis of FCRP and the presentation and discussion of the results obtained by the application of the first and second formulations to FCRP with an aspect ratio $\alpha = 0{\cdot}6$. In the last section, the results obtained by the new approaches are discussed, to determine accurately the limit of validity of each formulation, via comparison with the previous known results.

2. REVIEW OF THE SEMI-ANALYTICAL METHOD FOR THE DETERMINATION OF THE NON-LINEAR MODE SHAPES AND RESONANCE FREQUENCIES OF FCRP AT LARGE VIBRATION AMPLITUDES

The objective of the present paper is to present an improvement of the semi-analytical model for non-linear free vibration of FCRP developed in references [6, 19, 21], in order to establish new explicit formulae, or reduced linear systems, allowing easy reproduction of the results given in these references, which have been obtained via numerical iterative solution of non-linear algebraic systems. We start by presenting in this section a brief review of the theory, which is reproduced here using Lagrange's equations, in order to make it easy for the reader to understand the notation and the analytical developments presented in the remainder of the paper.

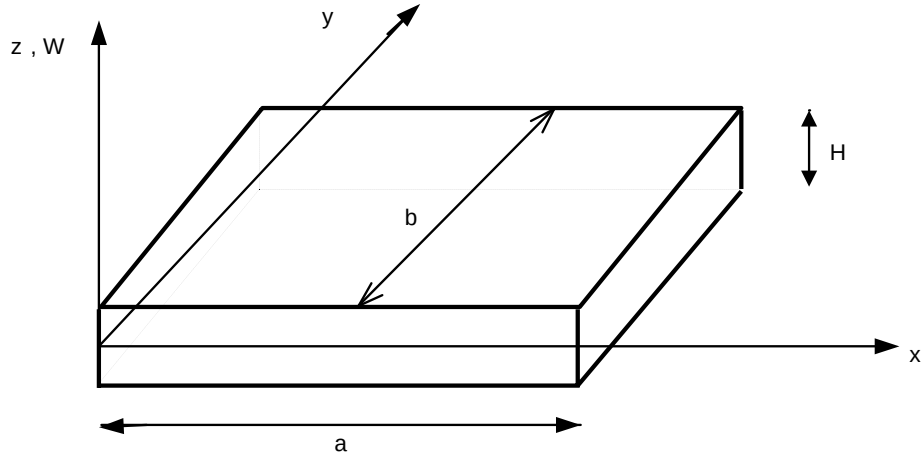

Figure 1. Plate notation.

Consider the transverse vibrations of the FCRP shown in Figure 1 and having the characteristics given in the Nomenclature. For such a plate, the strain energy V is given as the sum of the strain energy due to the bending V_b, and the membrane strain energy induced by large deflections V_a. In references [19, 21], the expressions used for V_b, V_a, and the kinetic energy T have been extensively discussed on the basis of a systematic comparison of the results obtained previously both experimentally and theoretically, based on various approaches. The approximate expressions adopted were

$$V_b = \frac{1}{2}\int_S D\left(\frac{\partial^2 W}{\partial x^2} + \frac{\partial^2 W}{\partial y^2}\right)^2 \mathrm{d}S, \qquad V_a = \frac{3D}{2H^2}\int_S \left[\left(\frac{\partial W}{\partial x}\right)^2 + \left(\frac{\partial W}{\partial y}\right)^2\right]^2 \mathrm{d}S, \quad (1, 2)$$

$$T = \frac{1}{2}\rho H \int_S \left(\frac{\partial W}{\partial t}\right)^2 \mathrm{d}S, \quad (3)$$

in which W is the transverse deflection function, S is the plate area, and V_b is the simplified bending strain energy expression, which is valid for the FCRP boundaries considered here [28].

In the above expressions, terms involving the in-plane displacements U and V and their derivatives, which are given, for example, in reference [28], have been omitted. This assumption has been made in references [19, 21] when calculating the first and second non-linear mode shapes of FCRP and its range of validity has been discussed in the light of the experimental and numerical results obtained for the non-linear frequency amplitude dependence and the non-linear bending stress estimates obtained at large vibration amplitudes. For the first non-linear mode shape, it was found that the percentage error in the non-linear frequency estimates based on this assumption, for amplitudes up to 1·5 the plate thickness, does not exceed 1·3%. On the other hand, the rate of increase in the bending stress estimates, obtained from measured data, was in good agreement with that obtained from the theory, in which the assumption of zero in-plane displacements was made [24]. For the second FCRP non-linear mode shape [19], the assumption of zero in-plane displacements has led to results which were in a very good agreement with those given in reference [16], based on the HFEM. Also, the effects of neglecting or taking into account the in-plane displacements U and V have been examined in the excellent discussion given in

reference [15], in which a cancellation effect, which explains the reasonable results obtained if U and V are taken equal to zero, has been noticed. As the purpose of the present work was the development of a direct and simple theory, valid for a reasonable range of vibration amplitudes, the assumption of zero in-plane displacements has been made as in references [19, 21]. Further investigations are being directed toward the development of more complex and complete formulations of the non-linear vibration problem, including the in-plane displacements, and other non-linear effects, such as the harmonic distortion, spatially distributed, which will be presented later.

Using a generalized parameterization and the usual summation convention used in reference [21], the transverse displacement of a point (x, y) of the plate mid-plane can be written as

$$W(x, y, t) = q_i(t)\, w_i(x, y). \tag{4}$$

Substituting W into expressions (1–3) for V_b, V_a, and T, and rearranging leads to

$$V_b = \tfrac{1}{2} q_i q_j k_{ij}, \quad V_a = \tfrac{1}{2} q_i q_j q_k q_l b_{ijkl}, \quad T = \tfrac{1}{2} \dot{q}_i \dot{q}_j m_{ij}, \tag{5–7}$$

in which m_{ij}, k_{ij} and b_{ijkl} are the general terms of the mass tensor, the rigidity tensor, and the non-linear rigidity tensor defined in references [6, 21] as

$$m_{ij} = \rho H \int_S w_i(x, y)\, w_j(x, y)\, \mathrm{d}x\, \mathrm{d}y, \tag{8}$$

$$k_{ij} = \int_S D\left(\frac{\partial^2 w_i}{\partial x^2} + \frac{\partial^2 w_i}{\partial y^2}\right)\left(\frac{\partial^2 w_j}{\partial x^2} + \frac{\partial^2 w_j}{\partial y^2}\right) \mathrm{d}x\, \mathrm{d}y, \tag{9}$$

$$b_{ijkl} = \frac{3D}{H^2} \int_S \left(\left(\frac{\partial w_i}{\partial x}\right)\left(\frac{\partial w_j}{\partial x}\right) + \left(\frac{\partial w_i}{\partial y}\right)\left(\frac{\partial w_j}{\partial y}\right)\right)\left(\left(\frac{\partial w_k}{\partial x}\right)\left(\frac{\partial w_l}{\partial x}\right) + \left(\frac{\partial w_k}{\partial y}\right)\left(\frac{\partial w_l}{\partial y}\right)\right) \mathrm{d}x\, \mathrm{d}y \tag{10}$$

and indices i, j, k and l are summed over $1, \ldots, n$.

The dynamic behaviour of the structure may be obtained by Lagrange's equations for a conservative system, which leads to

$$-\frac{\partial}{\partial t}\left(\frac{\partial T}{\partial \dot{q}_r}\right) + \frac{\partial T}{\partial q_r} - \frac{\partial V}{\partial q_r} = 0, \quad r = 1\text{–}n. \tag{11}$$

Replacing in this equation T and $V = (V_a + V_b)$ by their expressions given above leads to the following set of coupled non-linear differential equations, which is similar to that found in reference [22], and considered as a multi-dimensional form of the very well-known Duffing equation:

$$\ddot{q}_i m_{ir} + q_i k_{ir} + 2 q_i q_j q_k b_{ijkr} = 0, \quad r = 1, \ldots, n, \tag{12}$$

which can be written in the matrix form as

$$[\mathbf{M}]\{\ddot{\mathbf{q}}\} + [\mathbf{K}]\{\mathbf{q}\} + 2[\mathbf{B}(\{\mathbf{q}\})]\{\mathbf{q}\} = \{\mathbf{0}\}, \tag{13}$$

where $[\mathbf{M}]$, $[\mathbf{K}]$ and $[\mathbf{B}]$ are, respectively, the mass matrix, the linear rigidity matrix, and the geometrically non-linear rigidity matrix depending on the column vector of time-dependent generalized parameters $\{\mathbf{q}\}^{\mathrm{T}} = [q_1\, q_2 \ldots q_n]$.

The present work is concerned with the free response of FCRP with the objective of determining the spatial dependence of the non-linear mode shapes on the amplitude of vibration, which has been observed experimentally in the early paper of White [29], and carefully measured by Benamar *et al.* in reference [24]; and its consequences on the non-linear bending stress patterns. So, harmonic motion has been assumed as in references [19, 21]:

$$q_i(t) = a_i \cos(\omega t). \tag{14}$$

Substituting equation (14) into equation (13) and applying the harmonic balance method leads to

$$2([\mathbf{K}] - \omega^2[\mathbf{M}])\{\mathbf{A}\} + 3[\mathbf{B}(\mathbf{A})]\{\mathbf{A}\} = \{\mathbf{0}\}, \tag{15}$$

in which $\{\mathbf{A}\}$ is the column vector of the basic function contribution coefficients $\{\mathbf{A}\}^{\mathrm{T}} = [a_1 a_2 \dots a_n]$. To obtain non-dimensional parameters, we put, as in reference [21]:

$$w_i(x, y) = H w_i^*\left(\frac{x}{a}, \frac{y}{b}\right) = H w_i^*(x^*, y^*), \tag{16}$$

$$\frac{\omega^2}{\omega^{*2}} = \frac{D}{\rho H b^4}, \quad \frac{k_{ij}}{k_{ij}^*} = \frac{DaH^2}{b^3}, \quad \frac{m_{ij}}{m_{ij}^*} = \rho H^3 ab, \quad \frac{b_{ijkl}}{b_{ijkl}^*} = \frac{DaH^2}{b^3}. \tag{17–20}$$

Substituting these expressions into equation (15) leads to

$$([\mathbf{K}^*] - \omega^{*2}[\mathbf{M}^*])\{\mathbf{A}\} + \tfrac{3}{2}[\mathbf{B}^*(\mathbf{A})]\{\mathbf{A}\} = \{\mathbf{0}\} \tag{21}$$

which may also be written, using the tensor notation, as

$$-\omega^{*2} a_i m_{ir}^* + a_i k_{ir}^* + \tfrac{3}{2} a_i a_j a_k b_{ijkr}^* = 0, \quad r = 1\text{–}n. \tag{22}$$

Equation (22) is identical to that obtained in reference [21] for the non-linear vibrations of beams and plates using Hamilton's principle and integration of the time functions over the range $[0, 2\pi/\omega]$. These equations are a set of non-linear algebraic equations, involving the parameters m_{ij}^*, k_{ij}^* and b_{ijkl}^* which have been computed numerically by a routine called PREP [6]. In order to obtain the numerical solution for the non-linear problem in the neighbourhood of a given mode shape, the contribution of the dominant function participating in this mode was chosen and those of the other functions were calculated numerically. For example, for the first mode shape of a FCRP, the procedure consisted in fixing a_1, which is the contribution of the function w_{11}^* defined in section 3.1, and calculating the higher mode contributions a_r, $r = 2\text{–}n$, from the system

$$-\omega^{*2} a_i m_{ir}^* + a_i k_{ir}^* + \tfrac{3}{2} a_i a_j a_k b_{ijkr}^* = 0, \quad r = 2\text{–}n. \tag{23}$$

in which ω^{*2} is replaced by the expression obtained from the principle of conservation of energy, i.e.,

$$\omega^{*2} = \frac{a_i a_j k_{ij}^* + a_i a_j a_k a_l b_{ijkl}^*}{a_i a_j m_{ij}^*}. \tag{24}$$

Numerical data corresponding to the first two non-linear FCRP mode shapes have been computed and tabulated in references [19, 21] for a wide range of vibration amplitudes and different aspect ratios.

3. THE NEW APPROACH FOR DIRECT DETERMINATION OF THE GEOMETRICALLY NON-LINEAR FREE RESPONSE OF FCRP

3.1. INTRODUCTION

The purpose of this section is to extend the first and second formulations developed for beams in Part I of this series of papers in order to re-obtain the FCRP first and second non-linear mode shapes and the associated non-linear frequencies and bending stress patterns, at large vibration amplitudes, via simple explicit formulae, ready to use for engineering or analytical purposes, or via the solution of reduced linear systems of eight equations and eight unknowns. Then, comparison of the new results with the previous ones is made in order to determine accurately the limit of validity of each formulation. Analytical details are given in this section for the first FCRP non-linear mode shape. Results for the second non-linear mode shape obtained similarly are presented in sections 3.2.4 and 4.2.

Consider the large vibration amplitudes of the FCRP shown in Figure 1, having an aspect ratio $\alpha = b/a$, in the neighbourhood of its first resonant frequency. Following the choice of basic functions adopted in reference [21], the plate transverse deflections in the x and y directions are presented by clamped–clamped beam functions. So, the simple index k of the contribution a_k used in series expansion (4) for the plate deflection function $w_k(x, y)$, or its non-dimensional equivalent $w_k^*(x^*, y^*)$, may be replaced by a double index α_{ij}, which means that the plate function w_k is the product of the ith and jth clamped–clamped beam functions in the x and y directions respectively:

$$w^*(x^*, y^*) = a_k w_k^*(x^*, y^*) = \alpha_{ij} w_{ij}^*(x^*, y^*). \tag{25}$$

The relationship between the simple index k and the corresponding double indexes ij when using nine plate functions obtained as products of the first three beam functions in the x and y directions is

$$k = 3(i - 1) + j, \tag{26}$$

so that when i and j vary from 1 to 3, k varies from 1 to 9. In the remainder of this paper, either simple or double index notations will be used, depending on the context.

To determine the first non-linear mode shape of FCRP, the linear rigidity matrix k_{ij}^* and non-linear geometrical rigidity tensor b_{ijkl}^* have been calculated using the first nine symmetric–symmetric plate basic functions, obtained as products of the first three symmetric clamped–clamped beam mode shapes, given in Appendix A, in the x and y directions. This choice has been adopted because it leads to nine plate functions whose contributions to the first linear mode shape of fully clamped square plates have been shown to be significant in results, considered now as classical, published by Leissa from Young's work, based on Rayleigh–Ritz analysis [7, 8, 30]. Also, this conclusion has been confirmed in the non-linear case by the convergence study performed in reference [21], in which 36 plate functions have been used, for different plate aspect ratios, but only the contributions of the nine functions mentioned above have been found to be significant. For the second non-linear mode of FCRP having an aspect ratio α less than unity, it was shown similarly that the nine plate functions contributing significantly are those obtained by multiplying the first three antisymmetric clamped–clamped beam functions in the x direction by the first three symmetric clamped–clamped beam functions in the y direction [19].

To illustrate now the main idea behind the present approach, we present here in Table 1 data obtained via the iterative solution of the non-linear algebraic system (23) previously published in reference [21]. It can be seen from in this table, corresponding to the first non-linear mode shape of FCRP with an aspect ratio $\alpha = 0{\cdot}6$, that the contribution a_1 of the

TABLE 1

Contribution coefficients in the BFB to the first non-linear mode shape of a FCRP, obtained numerically from the iterative solution of the non-linear algebraic system, published in reference [21] ($\alpha = 0{\cdot}6$)

w^*_{max}	ω_{nl}/ω_l	a_{11}	a_{13}	a_{15}	a_{31}	a_{33}	a_{35}	a_{51}	a_{53}	a_{55}
0·1223	1·0027	0·05	0·2870E−03	0·4128E−04	0·1688E−02	−0·9539E−04	−0·1959E−04	0·2660E−03	−0·5795E−04	−0·1462E−04
0·2441	1·0108	0·10	0·6430E−03	0·1118E−03	0·3626E−02	−0·1723E−03	−0·4638E−04	0·5535E−03	−0·1183E−03	−0·2846E−04
0·3649	1·0239	0·15	0·1129E−02	0·2390E−03	0·6029E−02	−0·2123E−03	−0·8645E−04	0·8849E−03	−0·1822E−03	−0·4108E−04
0·4844	1·0417	0·20	0·1793E−02	0·4471E−03	0·9051E−02	−0·1971E−03	−0·1439E−03	0·1284E−02	−0·2487E−03	−0·5259E−04
0·6025	1·0636	0·25	0·2665E−02	0·7561E−03	0·1278E−01	−0·1091E−03	−0·2206E−03	0·1774E−02	−0·3144E−03	−0·6362E−04
0·7191	1·0893	0·30	0·3763E−02	0·1182E−02	0·1724E−01	0·6749E−04	−0·3164E−03	0·2375E−02	−0·3735E−03	−0·7507E−04
0·8344	1·1181	0·35	0·5089E−02	0·1735E−02	0·2241E−01	0·3460E−03	−0·4292E−03	0·3107E−02	−0·4191E−03	−0·8788E−04
0·9486	1·1499	0·40	0·6637E−02	0·2423E−02	0·2824E−01	0·7369E−03	−0·5560E−03	0·3980E−02	−0·4433E−03	−0·1028E−03
1·0619	1·1840	0·45	0·8396E−02	0·3251E−02	0·3465E−01	0·1247E−02	−0·6930E−03	0·5001E−02	−0·4381E−03	−0·1201E−03
1·1744	1·2203	0·50	0·1035E−01	0·4212E−02	0·4157E−01	0·1882E−02	−0·8359E−03	0·6172E−02	−0·3964E−03	−0·1398E−03
1·2864	1·2584	0·55	0·1248E−01	0·5323E−02	0·4892E−01	0·2640E−02	−0·9809E−03	0·7491E−02	−0·3117E−03	−0·1615E−03
1·5093	1·3392	0·65	0·1719E−01	0·7934E−02	0·6463E−01	0·4525E−02	−0·1262E−02	0·1054E−01	0·5518E−05	−0·2078E−03
1·7316	1·4251	0·75	0·2238E−01	0·1104E−01	0·8130E−01	0·6868E−02	−0·1510E−02	0·1408E−01	0·5390E−03	−0·2512E−03
1·9538	1·5151	0·85	0·2793E−01	0·1458E−01	0·9860E−01	0·9618E−02	−0·1705E−02	0·1802E−01	0·1296E−02	−0·2833E−03
2·1763	1·6085	0·95	0·3375E−01	0·1849E−01	0·1163E+00	0·1271E−01	−0·1836E−02	0·2228E−01	0·2269E−02	−0·2967E−03
2·3992	1·7046	1·05	0·3975E−01	0·2272E−01	0·1342E+00	0·1610E−01	−0·1894E−02	0·2678E−01	0·3442E−02	−0·2862E−03
3·4069	2·1630	1·50	0·6781E−01	0·4425E−01	0·2156E+00	0·3352E−01	−0·1272E−02	0·4858E−01	0·1058E−01	0·1114E−03
4·5320	2·7049	2·00	0·9936E−01	0·7030E−01	0·3055E+00	0·5457E−01	0·7031E−03	0·7362E−01	0·2042E−01	0·1141E−02

first basic function, which is the product of the first clamped–clamped beam linear mode shape in the x direction, with the first clamped–clamped beam linear mode shape in the y direction, remains predominant for the whole range of vibration amplitudes considered, compared to the contributions of the other functions. So, the contribution coefficient vector $\{\mathbf{A}\}$, defined in reference [21] by $\{\mathbf{A}\}^{\mathrm{T}} = [a_1 a_2 \dots a_9]$, can be written as $\{\mathbf{A}\}^{\mathrm{T}} = [a_1 \varepsilon_2 \dots \varepsilon_9]$ in which ε_i, representing the ith FCRP basic function contribution, may be considered as small, compared to a_1, for $i = 2$–9. Since the non-linearity parameters b_{ijkl} defined in equation (9) are of the same order of magnitude (see Appendix B), due to the above observation, some terms may be neglected in the non-linear expression $a_i a_j a_k b^*_{ijkr}$ in equation (22), which leads to two simple formulations, called in the remainder of this paper the first and the second formulation, defined in the next sections.

3.2. THE FIRST FORMULATION, LEADING TO EXPLICIT ANALYTICAL EXPRESSIONS FOR THE NON-LINEAR MODE SHAPES OF FCRP

3.2.1. *Formulation in the beam functions basis (BFB) and necessity of use of the modal function basis (MFB)*

The formulation presented in this section is said to be made in the beam functions basis, denoted in what follows as the BFB, since it is based on equation (23), in which the parameters m^*_{ij}, k^*_{ij} and b^*_{ijkl} are calculated from expressions (8–10), involving the basic functions w^*_i, defined in section 3.1, and obtained as products of beam functions.

The first formulation is based on an approximation which consists in neglecting in the expression $a_i a_j a_k b^*_{ijkr}$ of equation (23), which involves summation for the repeated indices i, j, k over the range $\{1,2, \dots, n\}$, both first and second order terms with respect to ε_i, i.e., terms of the type $a_1^2 \varepsilon_k b^*_{11kr}$, or of the type $a_1 \varepsilon_j \varepsilon_k b^*_{1jkr}$, so that the only remaining term is $a_1^3 b^*_{111r}$. This leads to

$$(k^*_{ir} - \omega^{*2} m^*_{ir}) \varepsilon_i + \tfrac{3}{2} a_1^3 b^*_{111r} = 0 \quad \text{for } r = 2, \dots, 9. \tag{27}$$

If k^*_{ir}, for $i \neq r$, is assumed to be negligible compared with k^*_{rr}, with the objective of obtaining an analytical solution, the above system permits one to obtain explicitly the basic function contributions $\varepsilon_2, \varepsilon_3, \dots, \varepsilon_9$ of the second and higher functions, corresponding to a given value of the assigned first basic function contribution a_1, as follows:

$$\varepsilon_r = -\frac{\frac{3}{2} a_1^3 b^*_{111r}}{(k^*_{rr} - \omega^{*2} m^*_{rr})} \quad (r = 2, 3, \dots, 9). \tag{28}$$

In equation (28), the ε_r's, for $r > 1$, depend on the classical parameters m^*_{rr}, k^*_{rr}, and the non-linear parameters b^*_{111r} calculated in the BFB. They depend also on the assigned first function contribution a_1, and the non-linear frequency parameter ω^*. On the other hand, the single mode approach gives a good estimate of the non-linear frequency parameter ω^* for maximum plate displacement amplitudes up to 1·34 times the plate thickness, as may be seen from Figure 2, in which the non-linear frequency estimates, calculated using the single function formula (29) given below, and the complete formula (24), are plotted against the maximum non-dimensional displacement amplitude $w^*_{\max}$, obtained at the plate centre. Consequently, ω^{*2} may be estimated, in the range of displacement amplitudes considered, with a percentage error below 3%, compared with equation (24), by

$$\omega^{*2} = \frac{k^*_{11}}{m^*_{11}} + \frac{b^*_{1111}}{m^*_{11}} a_1^2. \tag{29}$$

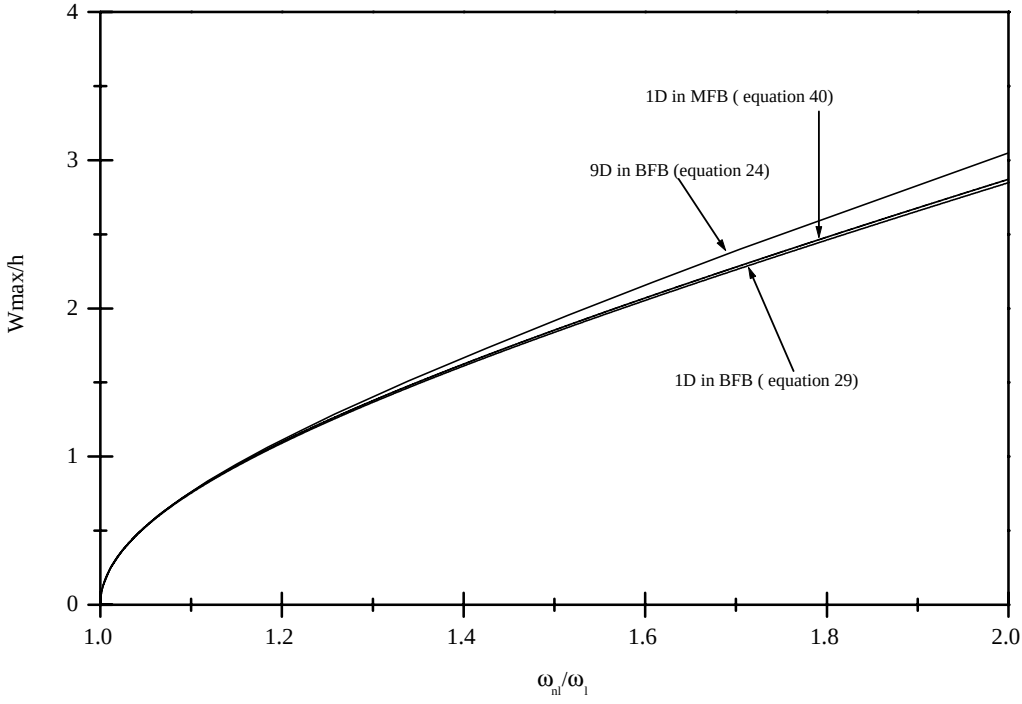

Figure 2. Comparison of the single function formula, for the non-linear frequency parameter, ω_{nl}/ω_l written in the BFB, i.e., equation (29), and in the MFB, i.e., equation (40), with the multi-mode formula (equation (24)).

Substituting equation (29) into equation (28) leads to

$$\varepsilon_r = \frac{3a_1^3 b^*_{r111}}{2((k^*_{11} + a_1^2 b^*_{1111})\dfrac{m^*_{rr}}{m^*_{11}} - k^*_{rr})} \quad (r = 2,3,\ldots,9) \tag{30}$$

As the normalization procedure applied in reference [21] to the elements of the BFB leads to a mass matrix identical to the identity matrix, m^*_{11} and m^*_{rr} are equal to 1 and equation (28) may be simplified to

$$\varepsilon_r = \frac{3a_1^3 b^*_{r111}}{2(k^*_{11} + a_1^2 b^*_{1111} - k^*_{rr})} \quad (r = 2, 3, \ldots, 9). \tag{31}$$

Expression (31) is an explicit simple formula, allowing calculation in the BFB of the higher function contributions to the first non-linear FCRP mode shape, as functions of the assigned first function contribution a_1, and of the known parameters k^*_{rr}, m^*_{rr} and b^*_{111r} (given in Appendix B).

In Table 2, numerical results for the basic function contributions to the fundamental non-linear mode shape of FCRP with an aspect ratio $\alpha = 0{\cdot}6$, based on the first formulation applied in the BFB, and calculated using equation (31), are summarized. A comparison between Table 2 and Table 1 shows notable differences between contributions. These differences can be explained as follows: in the beam cases presented in reference [20], the bases used to expand the displacement function series were those of the linear normal modes of vibration of the beam considered in each case, in which the mass and rigidity matrices are diagonal. In the FCRP case considered here, the basic functions used in the

TABLE 2

Contribution coefficients in the BFB to the first non-linear mode shape of a FCRP, calculated via the explicit expressions obtained from application of the first formulation in the BFB ($\alpha = 0{\cdot}6$)

w^*_{max}	ω_{nl}/ω_l	a_{11}	a_{13}	a_{15}	a_{31}	a_{33}	a_{35}	a_{51}	a_{53}	a_{55}
0·12598149 E+00	0·100273E+01	0·5000000 E−01	0·1433550 E−04	0·5217108 E−05	0·5498663 E−04	0·8078420 E−06	−0·188534 E−05	0·2660310 E−05	−0·108640 E−05	0·3222832 E−06
0·25118467 E+00	0·101081E +01	0·100000E +00	0·1147758 E−03	0·4174233 E−04	0·4419214 E−03	0·6466099 E−05	−0·150844 E−04	0·2130097 E−04	−0·869360 E−05	0·2578469 E−05
0·37480756 E+00	0·102388E +01	0·150000E +00	0·3878857 E−03	0·1409111 E−03	0·1503036 E−02	0·2184203 E−04	−0·509191 E−04	0·7199500 E−04	−0·293540 E−04	0·8703485 E−05
0·49599940 E+00	0·104142E +01	0·200000E +00	0·9211556 E−03	0·3341137 E−03	0·3601805 E−02	0·5183671 E−04	−0·120727 E−03	0·1710018 E−03	−0·696237 E−04	0·2063429 E−04
0·61383224 E+00	0·106287E +01	0·250000E +00	0·1803476 E−02	0·6528225 E−03	0·7135336 E−02	0·1014022 E−03	−0·235873 E−03	0·3348636 E−03	−0·136093 E−03	0·4031094 E−04
0·72726728 E+00	0·108773E+01	0·300000E+00	0·3125632 E−02	0·1128619 E−02	0·1254911 E−01	0·1755593 E−03	−0·407753 E−03	0·5805044 E−03	−0·235402 E−03	0·6967757 E−04

deflection function expansions have been calculated as products of x- and y-beam functions, as explained in section 3.1. Although the dominant component of the first and second linear FCRP mode shapes with an aspect ratio less than unity are $w^*_{11}(x^*, y^*)$ and $w^*_{21}(x^*, y^*)$, respectively, these functions do not coincide exactly with the FCRP first and second normal modes of vibration, and the corresponding rigidity matrices are not diagonal (cf., Appendix B). It is then necessary to make a change of basis, and formulate the problem on the basis of the linear mode shapes of the FCRP considered, called in the remainder of this paper the modal functions basis, and denoted as the MFB, in order to develop an explicit analytical solution of the problem. The linear diagonal rigidity matrix, corresponding to the first nine FCRP linear mode shapes, symmetric in both the x and y directions, in the MFB is given in Appendix B. It will be shown in sections 4.1 and 4.2 that the use of the MFB will lead to much more accurate values for the basic function contributions to the first and second FCRP non-linear mode shapes.

3.2.2. *Formulation of the FCRP non-linear free vibration problem in the modal functions basis (MFB)*

It appeared in the last section that the first formulation leads to poor results in the BFB. The purpose of the present section is to reformulate the FCRP non-linear free vibration problem in the MFB, in which the results obtained via the new formulations developed in the present paper will be found much more accurate, as will be shown in section 4. To do so, the expansion of the transverse displacement function $w^*(x^*, y^*)$ in the form of the finite series:

$$w^*(x^*, y^*) = a_k w^*_k(x^*, y^*) \tag{32}$$

given in equation (25) is rewritten as

$$w^*(x^*, y^*) = \bar{a}_k \phi^*_k(x^*, y^*), \tag{33}$$

where a summation is performed for the index k over the range $\{1, \ldots, n\}$ in both cases, and $\phi^*_k(x^*, y^*)$is the k^{th} symmetric–symmetric FCRP linear mode shape, denoted in what follows as the k^{th} SSFCRP linear mode shape, which is obtained from the numerical solution of the linear eigenvalue problem:

$$-\omega^{*2} a_i m^*_{ir} + a_i k^*_{ir} = 0, \quad r = 1\text{–}n, \tag{34}$$

performed using the software MATLAB.

Using the new notation, corresponding to the MFB, the non-linear algebraic system (23) may be written as

$$-\omega^{*2} \bar{a}_s \bar{m}^*_{sr} + \bar{a}_s \bar{k}^*_{sr} + \tfrac{3}{2}\, \bar{a}_s \bar{a}_u \bar{a}_v \bar{b}^*_{suvr} = 0, \quad r = 2\text{–}n \tag{35}$$

with ω^{*2} given by

$$\omega^{*2} = \frac{\bar{a}_r \bar{a}_s \bar{k}^*_{rs} + \bar{a}_r \bar{a}_s \bar{a}_u \bar{a}_v \bar{b}^*_{rsuv}}{\bar{a}_r \bar{a}_s \bar{m}^*_{rs}}, \tag{36}$$

in which the diagonal mass and rigidity matrices general terms $\bar{k}^*_{rs}$ and $\bar{m}^*_{rs}$, and the non-linear rigidity tensor $\bar{b}^*_{rsuv}$ are calculated in the MFB, using the formulae established in Appendix C.

3.2.3. *Application of the first formulation in the MFB to obtain explicit analytical expressions for the FCRP first non-linear mode shape*

The first formulation, developed now in the MFB, is based, like in section 3.1.2, on an approximation which consists in assuming that the contribution vector $\{\bar{\mathbf{A}}\}^{\mathrm{T}} = [\bar{a}_1 \bar{a}_2 \dots \bar{a}_n]$ can be written as $\{\bar{\mathbf{A}}\}^{\mathrm{T}} = [\bar{a}_1 \bar{\varepsilon}_2 \dots \bar{\varepsilon}_n]$, with $\bar{\varepsilon}_r$ being small compared to $\bar{a}_1$, for $r = 2, \dots, n$. Then, both first and second order terms with respect to $\bar{\varepsilon}_i$, i.e., terms of the type $\bar{a}_1^2 \bar{\varepsilon}_v \bar{b}^*_{11vr}$, or of the type $\bar{a}_1 \bar{\varepsilon}_u \bar{\varepsilon}_v \bar{b}^*_{1uvr}$ are neglected, so that the only remaining term is $\bar{a}_1^3 \bar{b}^*_{111r}$ in the expression $\bar{a}_s \bar{a}_u \bar{a}_v \bar{b}^*_{suvr}$ of equation (35), which becomes

$$(\bar{k}^*_{ir} - \omega^{*2} \bar{m}^*_{ir}) \bar{\varepsilon}_i + \tfrac{3}{2} \bar{a}_1^3 \bar{b}^*_{111r} = 0 \quad \text{for } r = 2, 3, \dots, 9, \tag{37}$$

in which the repeated index i should be summed over the range $\{1,2,\dots,9\}$. However, since use of the FCRP linear mode shapes as basic functions leads to diagonal mass and rigidity matrices, equation (37) can be written as

$$(\bar{k}^*_{rr} - \omega^{*2} \bar{m}^*_{rr}) \bar{\varepsilon}_r + \tfrac{3}{2} \bar{a}_1^3 \bar{b}^*_{111r} = 0 \quad \text{for } r = 2, 3, \dots, 9, \tag{38}$$

in which no summation is involved. The above system permits one to obtain explicitly the modal contributions $\bar{\varepsilon}_2, \bar{\varepsilon}_3, \dots, \bar{\varepsilon}_9$, in the MFB, of the second and higher basic functions, which are in the present case the higher linear mode shapes of the FCRP considered, corresponding to a given value $\bar{a}_1$ of the assigned first basic function contribution, i.e., the first FCRP linear mode shape, as follows:

$$\bar{\varepsilon}_r = -\frac{\frac{3}{2} \bar{a}_1^3 \bar{b}^*_{111r}}{(\bar{k}^*_{\mathrm{rr}} - \omega^{*2} \bar{m}^*_{rr})} \quad (r = 2, 3, \dots, 9). \tag{39}$$

In the above equation, the $\bar{\varepsilon}_r$'s, for $r > 1$, depend on the classical modal parameters $\bar{m}^*_{rr}$, $\bar{k}^*_{rr}$, the non-linear modal parameters $\bar{b}^*_{111r}$, the assigned first mode contribution $\bar{a}_1$, and the non-linear frequency parameter ω^*.

On the other hand, the single mode approach gives also in the MFB an accurate estimate of the non-linear frequency parameter $\omega^*$for high amplitudes, as may be seen from Figure 2. For displacement amplitudes up to 1.34 times the plate thickness, ω^{*2} may be well estimated, with a percentage error below 2·2%, compared with equation (36), by

$$\omega^{*2} = \frac{\bar{k}^*_{11}}{\bar{m}^*_{11}} + \frac{\bar{b}^*_{1111}}{\bar{m}^*_{11}} \bar{a}_1^2. \tag{40}$$

Substituting equation (40) into equation (39) leads to

$$\bar{\varepsilon}_r = \frac{3 \bar{a}_1^3 \bar{b}^*_{r111}}{2((k^*_{11} + \bar{a}_1^2 \bar{b}^*_{1111}) \bar{m}^*_{rr}/\bar{m}^*_{11} - \bar{k}^*_{rr})} \quad (r = 2, 3, \dots, 9). \tag{41}$$

As the mass matrix is identical to the identity matrix, due to the normalization procedure applied to the eigenvectors obtained from equation (34), $\bar{m}^*_{11}$ and $\bar{m}^*_{rr}$ are equal to 1 and equation (41) may be simplified to

$$\bar{\varepsilon}_r = \frac{3 \bar{a}_1^3 \bar{b}^*_{r111}}{2(\bar{k}^*_{11} + \bar{a}_1^2 \bar{b}^*_{1111} - \bar{k}^*_{rr})} \quad (r = 2, 3, \dots, 9). \tag{42}$$

Expression (42) is an explicit simple formula, allowing direct calculation of the higher modal function contributions to the first non-linear FCRP mode shape, as functions of the assigned first modal function contribution $\bar{a}_1$, and of the known parameters $\bar{m}^*_{rr}$, $\bar{k}^*_{rr}$ and $\bar{b}^*_{r111}$ (given in Appendix B). This defines the first non-linear amplitude-dependent FCRP mode shape $w^*_{nl1}(x^*, y^*, \bar{a}_1)$, for a given assigned value $\bar{a}_1$ of the first modal function

contribution, as a series involving the plate modal parameters depending on the first nine SSFCRP modes shapes $\phi_1^*, \phi_2^*, \ldots, \phi_9^*$:

$$w_{nl1}^*(x^*, y^*, \bar{a}_1) = \bar{a}_1 \phi_1^*(x^*, y^*) + \frac{3\bar{a}_1^3 \bar{b}_{2111}^*}{2((\bar{k}_{11}^* + \bar{a}_1^2 \bar{b}_{1111}^*) - \bar{k}_{22}^*)} \phi_2^*(x^*, y^*) + \frac{3\bar{a}_1^3 \bar{b}_{3111}^*}{2((\bar{k}_{11}^* + \bar{a}_1^2 \bar{b}_{1111}^*) - \bar{k}_{33}^*)} \phi_3^*(\mathrm{x}^*, \mathrm{y}^*) + \cdots + \frac{3\bar{a}_1^3 \bar{b}_{9111}^*}{2((\bar{k}_{11}^* + \bar{a}_1^2 \bar{b}_{1111}^*) - \bar{k}_{99}^*)} \phi_9^*(x^*, y^*), \tag{43}$$

in which the predominant term, proportional to the FCRP first linear mode shape $\phi_1^*(x^*, y^*)$, is $\bar{a}_1 \phi_1^*(x^*, y^*)$; and other terms, proportional to the higher SSFCRP mode shapes $\phi_2^*(x^*, y^*), \ldots, \phi_9^*(x^*, y^*)$, are the corrections due to the non-linearity.

3.2.4. *Application of the first formulation in the MFB to obtain explicit analytical expressions for the FCRP second non-linear mode shape*

The FCRP second linear mode shape has been expressed in reference [8], in the case of an aspect ratio $\alpha = b/a$ less than unity, using nine functions (obtained as products of the first three antisymmetric by the first three symmetric clamped–clamped beam functions in the x and y directions respectively), i.e., w_{21}^*, w_{23}^*, w_{25}^*, w_{41}^*, w_{43}^*, w_{45}^*, w_{61}^*, w_{63}^* and w_{65}^*. In reference [19], it was shown that these functions are those which contribute significantly to the second non-linear mode shape of the FCRP considered. Following the analysis presented in the above section, in the light of the previously published results summarized in Table 3, the model presented here may be developed for the second FCRP non-linear mode shape either in the new function basis, denoted as the BFB′, made of the functions just mentioned above, or in the corresponding modal functions basis, denoted as the MFB′, made of the first nine FCRP linear mode shapes, which are antisymmetric in the x direction, and symmetric in the y direction, denoted in what follows as: $\phi_1^{*\prime}, \phi_2^{*\prime}, \ldots, \phi_9^{*\prime}$, and refereed to as the ASFCRP modes. Using this notation, an analysis identical to that developed in the previous sections may be performed, leading to the contributions $\bar{\varepsilon}_r'$ of the rth AS linear mode shape, to the first non-linear ASFCRP mode shape, given by

$$\bar{\varepsilon}_r' = \frac{3\bar{a}_1'^3 \bar{b}_{r111}'^*}{2(\bar{k}_{11}'^* + \bar{a}_1'^2 \bar{b}_{1111}'^* - \bar{k}_{rr}'^*)}. \tag{44}$$

Expression (44) is an explicit simple formula, allowing calculation of the higher AS modal function contributions to the second non-linear FCRP mode shape, or the first non-linear ASFCRP mode shape, as functions of the assigned first AS modal function contribution $\bar{a}_1'$, and of the known parameters $\bar{k}_{rr}'^*$ and $\bar{b}_{r111}'^*$ (given in Appendix B).

The second amplitude-dependent FCRP non-linear mode shape $w_{nl2}^*(x^*, y^*, \bar{a}_1')$ for a given assigned value $\bar{a}_1'$ of the first AS modal function contribution is given similarly by

$$w_{nl2}'^*(x^*, y^*, \bar{a}_1') = \bar{a}_1' \phi_1^{*\prime}(x^*, y^*) + \frac{3\bar{a}_1'^3 \bar{b}_{2111}'^*}{2((\bar{k}_{11}'^* + \bar{a}_1'^2 \bar{b}_{1111}'^*) - \bar{k}_{22}'^*)} \phi_2^{*\prime}(x^*, y^*) + \frac{3\bar{a}_1'^3 \bar{b}_{3111}'^*}{2((\bar{k}_{11}'^* + \bar{a}_1'^2 \bar{b}_{1111}'^*) - \bar{k}_{33}'^*)} \phi_3^{*\prime}(x^*, y^*) + \cdots + \frac{3\bar{a}_1'^3 \bar{b}_{9111}'^*}{2((\bar{k}_{11}'^* + \bar{a}_1'^2 \bar{b}_{1111}'^*) - \bar{k}_{99}'^*)} \phi_9^{*\prime}(x^*, y^*). \tag{45}$$

TABLE 3

Contribution coefficients in the BFB to the second non-linear mode shape of a FCRP, obtained numerically from the iterative solution of the non-linear algebraic system, published in reference [19] ($\alpha = 0{\cdot}6$)

w^*_{max}	ω_{nl}/ω_l	a_{21}	a_{23}	a_{25}	a_{41}	a_{43}	a_{45}	a_{61}	a_{63}	a_{65}
0·116951	1·0035	0·05	0·9592E−03	0·1404E−03	0·1345E−02	−0·1188E−03	−0·3003E−04	0·2691E−03	−0·6280E−04	−0·2482E−04
0·232905	1·0138	0·10	0·2073E−02	0·3112E−03	0·3108E−02	−0·2313E−03	−0·5638E−04	0·5291E−03	−0·8882E−04	−0·5781E−04
0·347148	1·0305	0·15	0·3475E−02	0·5416E−03	0·5588E−02	−0·3275E−03	−0·7535E−04	0·7843E−03	−0·4413E−04	−0·1055E−03
0·459498	1·0530	0·20	0·5260E−02	0·8580E−03	0·8924E−02	−0·3940E−03	−0·8329E−04	0·1055E−02	0·1005E−03	−0·1715E−03
0·569933	1·0807	0·25	0·7488E−02	0·1283E−02	0·1311E−01	−0·4162E−03	−0·7670E−04	0·1368E−02	0·3688E−03	−0·2566E−03
0·678659	1·1130	0·30	0·1018E−01	0·1834E−02	0·1805E−01	−0·3811E−03	−0·5243E−04	0·1749E−02	0·7788E−03	−0·3583E−03
0·785952	1·1493	0·35	0·1333E−01	0·2524E−02	0·2362E−01	−0·2800E−03	−0·7929E−05	0·2218E−02	0·1343E−02	−0·4720E−03
0·892088	1·1890	0·40	0·1691E−01	0·3359E−02	0·2970E−01	−0·1087E−03	0·5854E−04	0·2781E−02	0·2068E−02	−0·5918E−03
0·997705	1·2317	0·45	0·2088E−01	0·4341E−02	0·3615E−01	0·1327E−03	0·1479E−03	0·3441E−02	0·2956E−02	−0·7109E−03
1·10271	1·2772	0·50	0·2519E−01	0·5470E−02	0·4289E−01	0·4409E−03	0·2601E−03	0·4193E−02	0·4004E−02	−0·8229E−03
1·20720	1·3249	0·55	0·2981E−01	0·6739E−02	0·4984E−01	0·8106E−03	0·3945E−03	0·5029E−02	0·5207E−02	−0·9218E−03
1·41526	1·4263	0·65	0·3974E−01	0·9670E−02	0·6413E−01	0·1708E−02	0·7244E−03	0·6920E−02	0·8035E−02	−0·1061E−02
1·62326	1·5342	0·75	0·5037E−01	0·1306E−01	0·7869E−01	0·2770E−02	0·1124E−02	0·9041E−02	0·1135E−01	−0·1100E−02
1·83068	1·6473	0·85	0·6145E−01	0·1682E−01	0·9335E−01	0·3947E−02	0·1577E−02	0·1133E−01	0·1506E−01	−0·1027E−02
2·03815	1·7646	0·95	0·7280E−01	0·2088E−01	0·1080E+00	0·5200E−02	0·2069E−02	0·1373E−01	0·1907E−01	−0·8426E−03
2·24604	1·8853	1·05	0·8430E−01	0·2517E−01	0·1226E+00	0·6501E−02	0·2588E−02	0·1621E−01	0·2331E−01	−0·5534E−03
3·18189	2·4590	1·50	0·1365E+00	0·4599E−01	0·1873E+00	0·1254E−01	0·5045E−02	0·2775E−01	0·4373E−01	0·1698E−02
4·22402	3·1314	2·00	0·1936E+00	0·6994E−01	0·2576E+00	0·1913E−01	0·7756E−02	0·4058E−01	0·6697E−01	0·5111E−02

Equation (45) defines the second non-linear amplitude-dependent FCRP mode shape $w^*_{nl2}(x^*, y^*, \bar{a}'_1)$, for a given assigned value $\bar{a}'_1$ of the first AS modal function contribution, as a series involving the plate modal parameters depending on the first nine antisymmetric–symmetric FCRP modes $\phi^{*\prime}_1, \phi^{*\prime}_2, \ldots, \phi^{*\prime}_9$, in which the predominant term, proportional to the second FCRP linear mode shape, or the first ASFCRP linear mode shape, is $\bar{a}'_1 \phi^{*\prime}_1(x^*, y^*)$; and the other terms, proportional to the higher ASFCRP mode shapes $\phi^{*\prime}_2(x^*, y^*), \ldots, \phi^{*\prime}_9(x^*, y^*)$, are the corrections due to the non-linearity.

3.3. THE SECOND FORMULATION, PERMITTING CALCULATION OF THE FCRP NON-LINEAR MODE SHAPES, VIA THE SOLUTION OF A LINEAR SYSTEM OF EIGHT EQUATIONS AND EIGHT UNKNOWNS, FOR EACH VALUE OF THE AMPLITUDE OF VIBRATION

As will be shown in sections 4.1.1 and 4.2, the explicit formulae established for the first and second non-linear FCRP mode shapes obtained via the first formulation developed in the above subsections yield accurate results for a relatively large range of vibration amplitudes. For higher amplitudes, a complementary formulation, called in the remainder of this paper the second formulation, may be considered, in which only second order terms of the type $\bar{a}_1 \bar{\varepsilon}_u \bar{\varepsilon}_v \bar{b}^*_{1uvr}$ are neglected when considering the first non-linear mode shape, in equation (35), corresponding to the non-linear free vibration problem formulated in the MFB, rewritten here for clarity as

$$-\omega^{*2} \bar{a}_s \bar{m}^*_{sr} + \bar{a}_s \bar{k}^*_{sr} + \tfrac{3}{2} \bar{a}_s \bar{a}_u \bar{a}_v \bar{b}^*_{suvr} = 0, \quad r = 2, 3, \ldots, 9. \tag{46}$$

Separating in the non-linear expression $\bar{a}_s \bar{a}_u \bar{a}_v \bar{b}^*_{suvr}$ terms proportional to $\bar{a}_1^3$, terms proportional to $\bar{a}_1^2 \bar{\varepsilon}_v$, and neglecting terms proportional to $\bar{a}_1 \bar{\varepsilon}_u \bar{\varepsilon}_v$ leads to

$$\bar{a}_s \bar{a}_u \bar{a}_v \bar{b}^*_{suvr} = \bar{a}_1^3 \bar{b}^*_{1\,1\,1\,r} + \bar{a}_1^2 \bar{\varepsilon}_v \bar{b}^*_{1\,1\,vr} \tag{47}$$

after substituting and rearranging, equation (46) can be written in matrix form as

$$([\bar{\mathbf{K}}^*_{RI}] - \omega^{*2} [\bar{\mathbf{M}}^*_{RI}]) \{\bar{\mathbf{a}}_{RI}\} + \tfrac{3}{2} [\boldsymbol{\alpha}^*_I] \{\bar{\mathbf{a}}_{RI}\} = \{ -\tfrac{3}{2} \bar{a}_1^3 \bar{b}^*_{i\,1\,1\,1} \}, \tag{48}$$

in which $[\bar{\mathbf{K}}^*_{RI}] = [\bar{\mathbf{k}}^*_{ij}]$ and $[\bar{M}^*_{RI}] = [\bar{m}^*_{ij}]$ are the reduced rigidity and mass matrices associated with the first FCRP non-linear mode shape, obtained by varying i and j in the set $\{2, 3, \ldots, 9\}$, $[\bar{\boldsymbol{\alpha}}^*_I]$ is an (8×8) square matrix, depending on $\bar{a}_1$, whose general term $\bar{\alpha}^*_{ij}$ is equal to $\bar{a}_1^2 \bar{b}^*_{ij\,1\,1}$; and $\{ -\tfrac{3}{2} \bar{a}_1^3 \bar{b}^*_{i\,1\,1\,1} \}$ is a column vector representing the right-hand side of linear system (48), in which the reduced unknown vector is $\{\bar{\mathbf{a}}_{RI}\}^T = [\bar{\varepsilon}_2 \bar{\varepsilon}_3 \ldots \bar{\varepsilon}_9]$. The modal function contributions $\bar{\varepsilon}_2, \bar{\varepsilon}_3, \ldots, \bar{\varepsilon}_9$ can be obtained very easily by solving linear system (48) of eight equations and eight unknowns for each assigned value of the first modal function contribution $\bar{a}_1$.

To obtain via the second formulation, the second non-linear FCRP mode shape, or the first non-linear ASFCRP mode shape, a linear system similar to equation (48) is written as

$$([\bar{\mathbf{K}}'^*_{RII}] - \omega^{*\prime 2} [\bar{\mathbf{M}}'^*_{RII}]) \{\bar{\mathbf{a}}'_{RII}\} + \tfrac{3}{2} [\boldsymbol{\alpha}'^*_{II}] \{\bar{\mathbf{a}}'_{RII}\} = \{ -\tfrac{3}{2} \bar{a}'^3_1 b_{i\,1\,1\,1} \}, \tag{49}$$

in which the general term of the matrix $[\bar{\boldsymbol{\alpha}}'^*_{II}]$ is equal to $\bar{a}'^2_1 \bar{b}'^*_{ij\,1\,1}$, $[\bar{\mathbf{K}}'^*_{RII}]$ and $[\bar{\mathbf{M}}'^*_{RII}]$ are reduced rigidity and mass matrices corresponding to the second FCRP non-linear mode shape, and $\{ -\tfrac{3}{2} \bar{a}'^3_1 b'^*_{i\,1\,1\,1} \}$ is a column vector representing the right-hand side of linear system (49) in which the reduced unknown vector is $\{\bar{\mathbf{a}}'_{RII}\}^T = [\bar{\varepsilon}'_2 \ldots \bar{\varepsilon}'_9]$. The modal function contributions can be obtained by solving a reduced linear system of eight equations and

eight unknowns. Higher FCRP non-linear mode shapes may be obtained in a similar manner, using appropriate reduced matrices in each case.

3.4. CONCLUSION

It appears from the two above subsections that the basic function contributions to the amplitude-dependent non-linear FCRP mode shapes may be calculated via the first formulation, developed in the MFB, i.e., the basis of the FCRP linear mode shapes, using simple explicit expressions involving the plate modal parameters $\bar{m}_{ij}^*$, $\bar{k}_{ij}^*$ and $\bar{b}_{ijkl}^*$. As will be shown in sections 4.1.1 and 4.2 in the light of the numerical results obtained, these simple expressions lead, in the case of FCRP with an aspect ratio $\alpha = 0{\cdot}6$, to accurate values for the basic function contributions, for maximum plate vibration amplitudes, reached at the plate centre $(x^*, y^*) = (0{\cdot}5, 0{\cdot}5)$, up to about 0·6 times the plate thickness, for the first non-linear FCRP mode shape. For the second non-linear mode shape, the domain of validity of the first formulation is restricted to maximum vibration amplitudes up to about 0·5 times the plate thickness, reached at $(x^*, y^*) = (0{\cdot}29, 0{\cdot}5)$. For higher amplitudes, more accurate results may be obtained in each case, based on the second formulation, via solution of a reduced linear system of eight equations and eight unknowns for each value of the amplitude of vibration. In the case of the first non-linear mode shape of the plates mentioned above, i.e., corresponding to $\alpha = 0{\cdot}6$, it is shown in section (4.1.2) that the second formulation leads to accurate results for maximum vibration amplitudes, up to about once the plate thickness.

4. PRESENTATION AND DISCUSSION OF THE NUMERICAL RESULTS OBTAINED BY APPLICATION OF THE NEW APPROACH TO THE FIRST AND SECOND NON-LINEAR MODE SHAPES OF FCRP WITH AN ASPECT RATIO $\alpha = 0{\cdot}6$

In this section, numerical results obtained from application of the theory presented above, to the first and second non-linear mode shapes of FCRP with an aspect ratio $\alpha = b/a = 0{\cdot}6$, are presented and discussed. Results corresponding to other aspect ratios, higher non-linear mode shapes, and the non-linear periodic forced response will be presented later.

4.1. FIRST NON-LINEAR MODE SHAPE OF FCRP WITH AN ASPECT RATION $\alpha = 0{\cdot}6$

4.1.1. *Explicit analytical expression for the first FCRP non-linear mode shape corresponding to* $\alpha = 0.6$

Replacing in equation (43) the FCRP modal parameters by their numerical values given in Appendix B, for an aspect ratio $\alpha = 0{\cdot}6$, leads to the following explicit expression for the first non-linear mode shape of this plate, involving nine terms:

$$w_{nl1}^*(x^*, y^*, \bar{a}_1) = \bar{a}_1 \phi_1^*(x^*, y^*) + \frac{913{,}69\bar{a}_1^3}{((670{\cdot}47 + 1461{\cdot}21\bar{a}_1^2) - 3242{\cdot}59)} \phi_2^*(x^*, y^*)$$

$$+ \frac{267{,}04\bar{a}_1^3}{((670{\cdot}47 + 1461{\cdot}21\bar{a}_1^2) - 14261.23)} \phi_3^*(x^*, y^*)$$

$$+\frac{1446{,}57\bar{a}_1^3}{((670{\cdot}47+1461{\cdot}21\bar{a}_1^2)-15483{\cdot}28)}\phi_4^*(x^*,y^*)$$

$$+\frac{-71{,}85\bar{a}_1^3}{((670{\cdot}47+1461{\cdot}21\bar{a}_1^2)-23475{\cdot}3)}\phi_5^*(x^*,y^*)$$

$$+\frac{303{,}78\bar{a}_1^3}{((670{\cdot}47+1461{\cdot}21\bar{a}_1^2)-45040{\cdot}81)}\phi_6^*(x^*,y^*)$$

$$+\frac{-3448{,}09\bar{a}_1^3}{((670{\cdot}47+1461{\cdot}21\bar{a}_1^2)-91294{\cdot}62)}\phi_7^*(x^*,y^*)$$

$$+\frac{1746{,}84\bar{a}_1^3}{((670{\cdot}47+1461{\cdot}21\bar{a}_1^2)-109581{\cdot}94)}\phi_8^*(x^*,y^*)$$

$$+\frac{-298{,}47\bar{a}_1^3}{((670{\cdot}47+1461{\cdot}21\bar{a}_1^2)-151664{\cdot}2)}\phi_9^*(x^*,y^*). \tag{50}$$

In which x^* and y^* are the non-dimensional geometrical co-ordinates defined in equation (16), which vary in the interval $[0,1]$, and $\phi_1^*, \phi_2^*, \ldots, \phi_9^*$ are the first nine SSFCRP linear mode shapes, whose components in the BFB are given in Appendix B.

The explicit expressions of equation (50) for the modal function contributions obtained via the first formulation, applied in the MFB, have been transposed to the BFB via the change of bases rule, in order to obtain the corresponding basic function contributions in the BFB, and enable comparisons to be made with the previous results, based on iterative solution of the non-linear algebraic system, previously published in reference [21]. The results summarized in Table 4 correspond to the values of $a_{13}, a_{15}, a_{31}, a_{33}, a_{35}, a_{51}, a_{53}, a_{55}$ obtained for some assigned values of a_{11} varying from 0·05 to 0·25, which correspond to maximum non-dimensional vibration amplitudes at the plate centre varying from 0·1223 to 0·5995. For each solution, the corresponding value of ω_{nl}/ω_l is also given. Comparison between Table 4 and Table 1, taken from reference [21], in which the basic function contributions have been calculated via iterative solution of the non-linear algebraic system (23), shows that the higher basic function contributions to the first non-linear FCRP mode shape obtained from the explicit expressions based on the first formulation, i.e., equation (50), are very close to those calculated via iterative solution of the non-linear algebraic system for finite amplitudes of vibration up to a maximum plate displacement amplitude equal to 0·6 times the plate thickness, which corresponds to $a_{11} \approx 0{\cdot}25$. For higher values of the vibration amplitude, slight differences start to appear and increase with the amplitude of vibration. This is illustrated in Figures 3–5, in which the basic function contributions of the most significantly contributing functions, i.e., a_{13}, a_{31} and a_{51}, expressed in the BFB, obtained from application of the first and second formulations in the MFB, are plotted versus the maximum non-dimensional plate vibration amplitude $w^*_{\max}$, obtained at the plate centre, and compared with the exact numerical solution. To have an accurate conclusion concerning the limit of validity of the first explicit solution, i.e., equation (50), in engineering applications, a criterion based on the effect of the differences appearing in the estimated basic function contributions to physical quantities, such as the non-linear frequency, the maximum plate non-linear bending stress, and the bending stress distribution in sensible regions of the plate has been adopted. The expressions used for the non-linear bending stress distribution associated with a given non-linear mode shape are given in Appendix D. It was found, as may be seen in Figure 6 and Table 5 respectively, that for amplitudes of

TABLE 4

Contribution coefficients in the BFB to the first non-linear mode shape of a FCRP, calculated via the explicit expressions obtained from application of the first formulation in the MFB, i.e., equation (50)*, and use of the change of based rule, to obtain the corresponding basic functions contributions in the BFB* ($\alpha = 0{\cdot}6$)

w^*_{max}	ω_{nl}/ω_l	a_{11}	a_{13}	a_{15}	a_{31}	a_{33}	a_{35}	a_{51}	a_{53}	a_{55}
0·122325E+00	0·100271E+01	0·500010E−01	0·287073E−03	0·412773E−04	0·168996E−02	−0·954032E−04	−0·196109E−04	0·266182E−03	−0·580222E−04	−0·146400E−04
0·244140E+00	0·101078E+01	0·100032E+00	0·645960E−03	0·112363E−03	0·364988E−02	−0·172176E−03	−0·467079E−04	0·554102E−03	−0·118865E−03	−0·284080E−04
0·364618E+00	0·102389E+01	0·150003E+00	0·114791E−02	0·242908E−03	0·615257E−02	−0·211199E−03	−0·886716E−04	0·885014E−03	−0·185209E−03	−0·404030E−04
0·483341E+00	0·104165E+01	0·200004E+00	0·186666E−02	0·463073E−03	0·949605E−02	−0·192875E−03	−0·152956E−03	0·128185E−02	−0·260000E−03	−0·497772E−04
0·599523E+00	0·106357E+01	0·250000E+00	0·287626E−02	0·802985E−03	0·139994E−01	−0·963603E−04	−0·246844E−03	0·176763E−02	−0·346068E−03	−0·556598E−04
0·712404E+00	0·108921E+01	0·300001E+00	0·425330E−02	0·129328E−02	0·200238E−01	0·100768E−03	−0·377550E−03	0·236691E−02	−0·446381E−03	−0·572030E−04

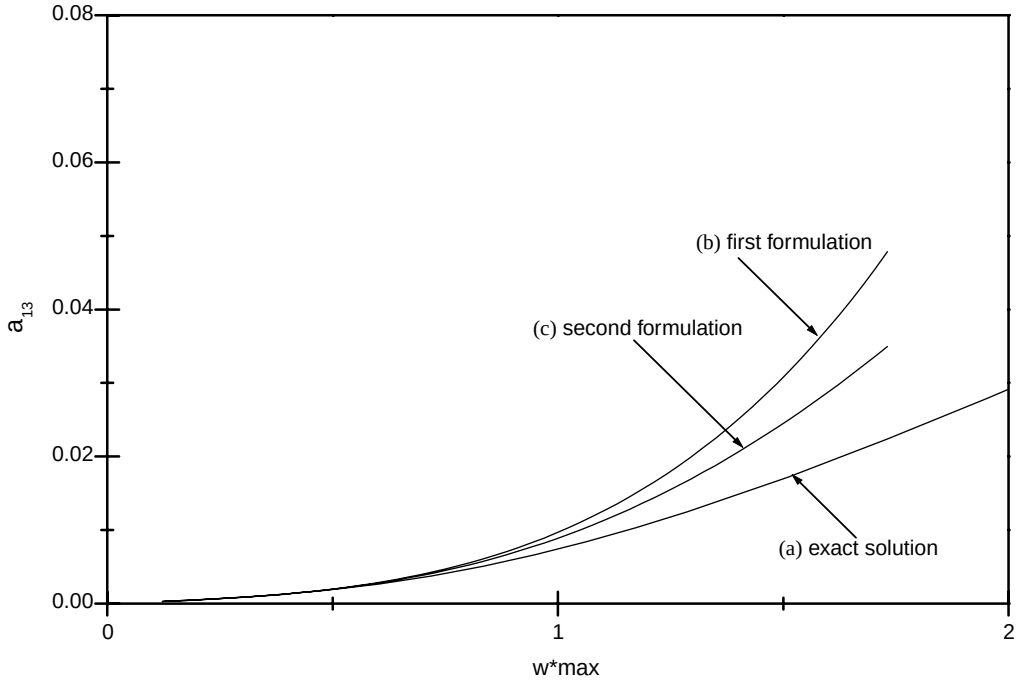

Figure 3. Comparison between the values of the contribution a_{13} to the first non-linear mode shape of a FCRP with an aspect ratio ($\alpha = 0{\cdot}6$) obtained by: (a) non-linear algebraic equations, (b) first formulation, and (c) second formulation.

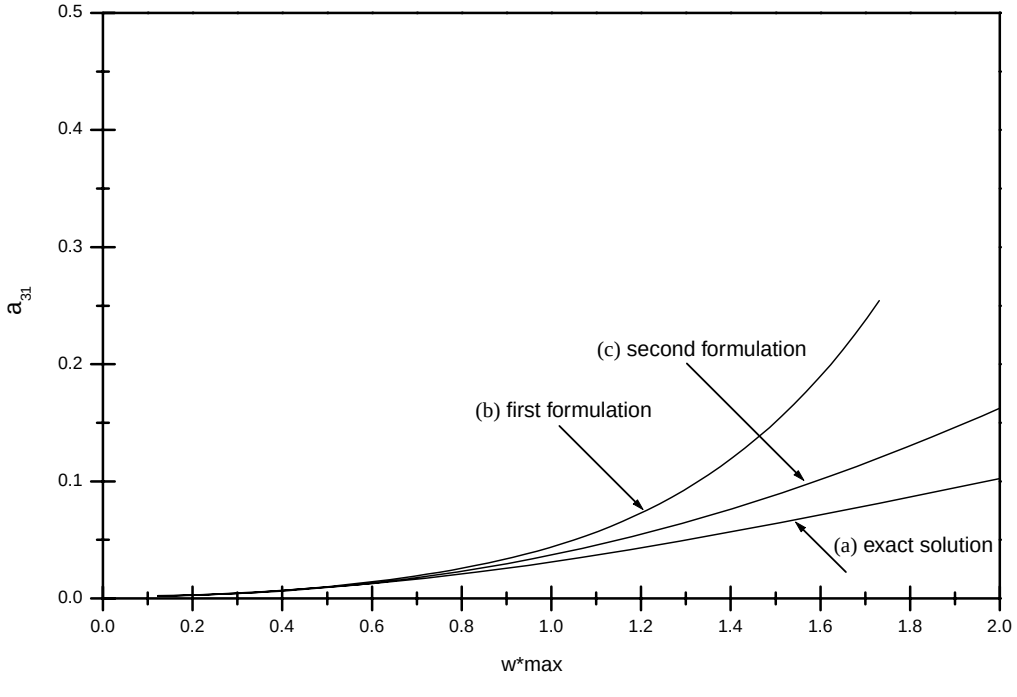

Figure 4. Comparison between the values of the contribution a_{31} to the first non-linear mode shape of a FCRP with an aspect ratio ($\alpha = 0{\cdot}6$) obtained by: (a) non-linear algebraic equations, (b) first formulation, and (c) second formulation.

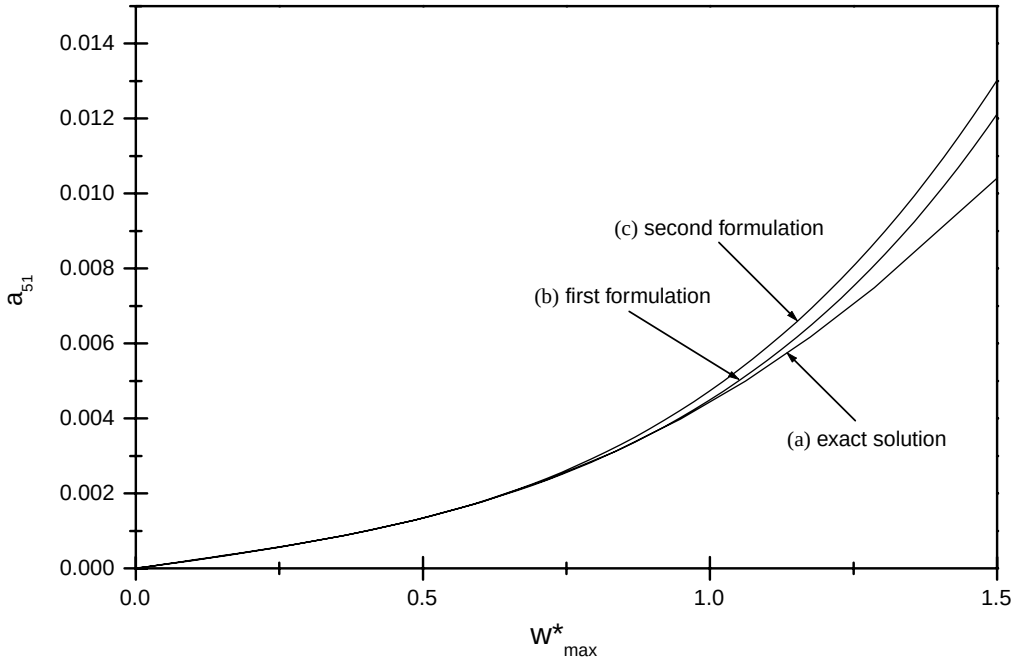

Figure 5. Comparison between the values of the contribution a_{51} to the first non-linear mode shape of a FCRP with an aspect ratio ($\alpha = 0{\cdot}6$) obtained by: (a) non-linear algebraic equations, (b) first formulation, and (c) second formulation.

TABLE 5

Comparison between the values of the non-dimensional stresses σ^*_{yo} $(0{\cdot}25, 0)$, *associated with the first non-linear mode shape of a FCRP with an aspect ratio* $\alpha = 0{\cdot}6$ *calculated using*: (a) *the exact solution of the non-linear algebraic system, i.e., equation* (23), (b) *the first formulation, i.e., equation* (42) *and* (c) *the second formulation, i.e., equation* (48)

w^*_{max}	Non-linear equations (I)	First formulation (II)	Second formulation (III)	Percentage (I and II)	Percentage (I and III)
0·1223	2·0739	2·0741	2·0740	0·0096%	0·0048%
0·2441	4·1924	4·1958	4·1946	0·081%	0·052%
0·3649	6·3962	6·4085	6·4047	0·192%	0·133%
0·4844	8·7191	8·7648	8·7470	0·52%	0·32%
0·6025	11·1869	11·3144	11·2615	1·14%	0·67%
0·7191	13·8171	14·1127	13·9811	2·14%	1·19%
0·8344	16·6198	17·2190	16·9371	3·6%	1·9%
0·9486	19·5992	20·7001	20·1549	5·62%	2·84%
1·0619	22·7549	24·6310	23·6547	8·24%	3·95%
1·1744	26·0828	29·1006	27·4531	11·57%	5·25%
1·2864	29·5765	34·2094	31·5652	15·66%	6·72%
1·5093	37·0271	46·8926	40·7574	26·64%	10·07%
1·7316	45·0315	64·1838	51·2757	42·53%	13·87%
1·9538	53·5101	88·9218	63·1203	66·18%	17·96%
2·1763	62·3868	127·9688	76·2714	105·12%	22·26%
2·3992	71·5925	210·8172	90·6849	194·47%	26·67%
3·4069	115·657		169·5205		46·57%

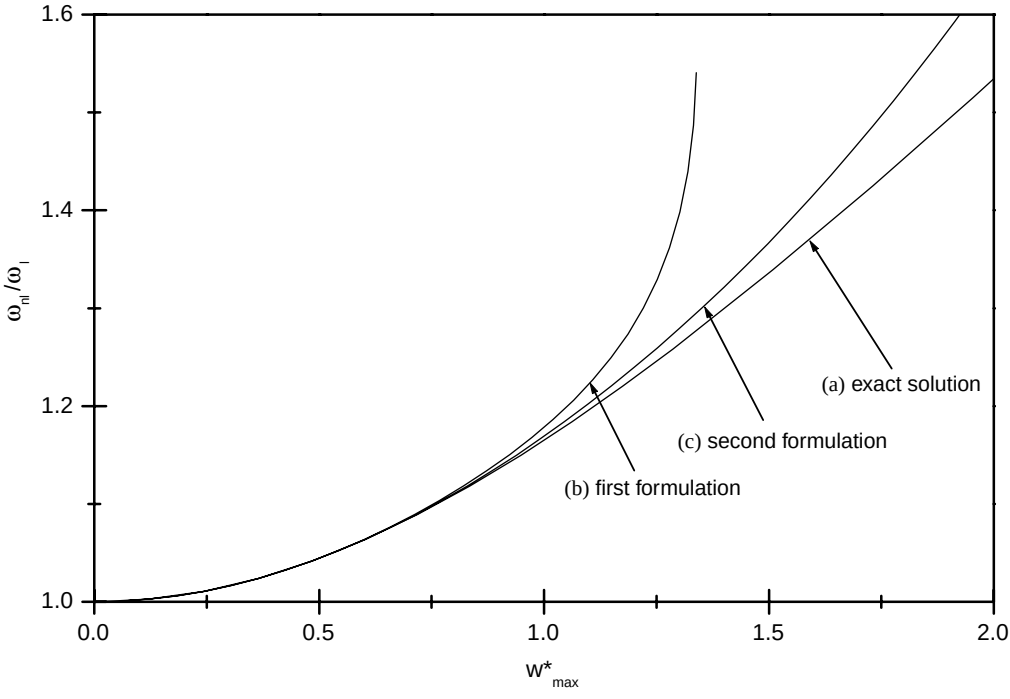

Figure 6. Comparison between frequency parameter ω_{nl}/ω_l, associated with the first non-linear SSFCRP mode shape, obtained by: (a) non-linear algebraic equations, (b) first formulation, and (c) second formulation.

vibration up to the plate thickness, the error induced by the first formulation does not exceed 0·066% for the non-linear frequency, and 5·62% for the maximum associated non-linear bending stress, determined numerically, and obtained at point (0·25,0). In Figure 7, the bending stress σ^*_{yb}, calculated at point (0·25, 0) by different methods, is plotted against the maximum non-dimensional amplitude of vibration w^*_{max}. This particular point has been chosen in the region in which the maximum value of σ^*_{yb} is reached, with the objective of illustrating the effect of the various approximations adopted. It can be seen from this figure that the first formulation can give a good approximation for the values of the bending stress for relatively high amplitudes of vibration. The difference between the exact value and that based on the first formulation does not exceed 5% for $w^*_{max} \approx 0{\cdot}9$.

The non-dimensional bending stress distribution associated with the FCRP first non-linear mode shape is plotted against y^* in Figure 8, for $x^* = 0{\cdot}25$, $\alpha = 0{\cdot}6$, and different values of the amplitude of vibration. It can be seen from this figure, corresponding to a region in which the maximum non-dimensional bending stress associated with the first non-linear mode shape is reached, that for the smallest non-dimensional amplitude considered, i.e., $w^* = 0{\cdot}1223$, the results based on the first formulation coincide with the solution obtained by the iterative procedure. For a maximum non-dimensional vibration amplitude $w^* = 0{\cdot}9486$, the maximum difference between the two curves is reached at $y^* = 0$, and is approximately 5%. For a maximum non-dimensional amplitude $w^* = 1{\cdot}5093$, the difference is approximately 25%. Figure 9 shows that for relatively small amplitudes, up to $w^*_{max} \approx 0{\cdot}5$, the first formulation gives a very good approximation for the bending stress $\sigma^*_{yb}(0{\cdot}275, y^*)$. For higher maximum amplitudes of vibration, some differences between the first formulation and the iterative solution may be noticed, with a maximum percentage of difference of 25% corresponding to $w^*_{max} \approx 1{\cdot}5$

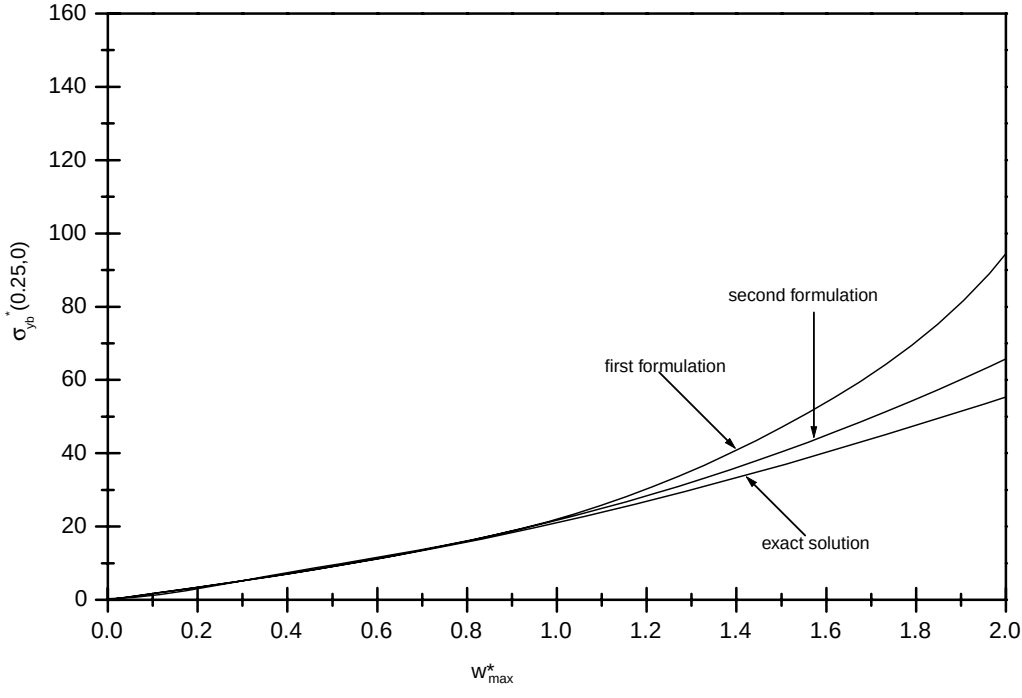

Figure 7. Non-dimensional bending stress σ^*_{yb} calculated at point (0·25, 0) and associated with the first non-linear mode shape of a FCRP with an aspect ratio $\alpha = 0{\cdot}6$.

4.1.2. *First non-linear mode shape of FCRP with an aspect ratio* $\alpha = 0{\cdot}6$ *obtained via the second formulation, from solution of a linear system of eight equations and eight unknowns for each value of the amplitude of vibration*

In Table 6, the modal function contributions to the first non-linear mode shape of FCRP with an aspect ratio $\alpha = 0.6$, calculated via the second formulation developed in section 3.3 are summarized. It may be noticed from comparison of this table with that obtained via iterative solution of the non-linear algebraic system, i.e., Table 1, and from Figures 3–5, that the corresponding intervals of validity largely exceed those obtained via the first formulation, and can reach vibration amplitudes up to once the plate thickness for the first FCRP non-linear mode shape.

In Figure 7 the bending stress σ^*_{yb} calculated at point (0·25, 0) by different methods is plotted against the maximum non-dimensional amplitude of vibration w^*_{max}. It can be seen that the second formulation gives, at this particular point, a good approximation for the values of the bending stress, the difference between the exact value and the second formulation does not exceed 10% for $w^*_{max} \approx 1{\cdot}5$.

In Figures 10 and 11, the distribution of the non-dimensional bending stress σ^*_{yb} is plotted against y^* for two sections corresponding to $x^* = 0{\cdot}275$ and 0·325 for a maximum non-dimensional amplitude of vibration $w^*_{max} \approx 1.5$. For the first section, the maximum percentage of difference is about 25 and 10% for the first and second formulations respectively. For the second section, the maximum percentage of difference is approximately 17% for the first formulation and 8·5% for the second formulation. Also, from Figure 12, it may be seen that the second formulation gives a non-dimensional bending stress distribution $\sigma^*_{yb}(0{\cdot}325, y^*)$ which is very close to that calculated by the iterative solution of

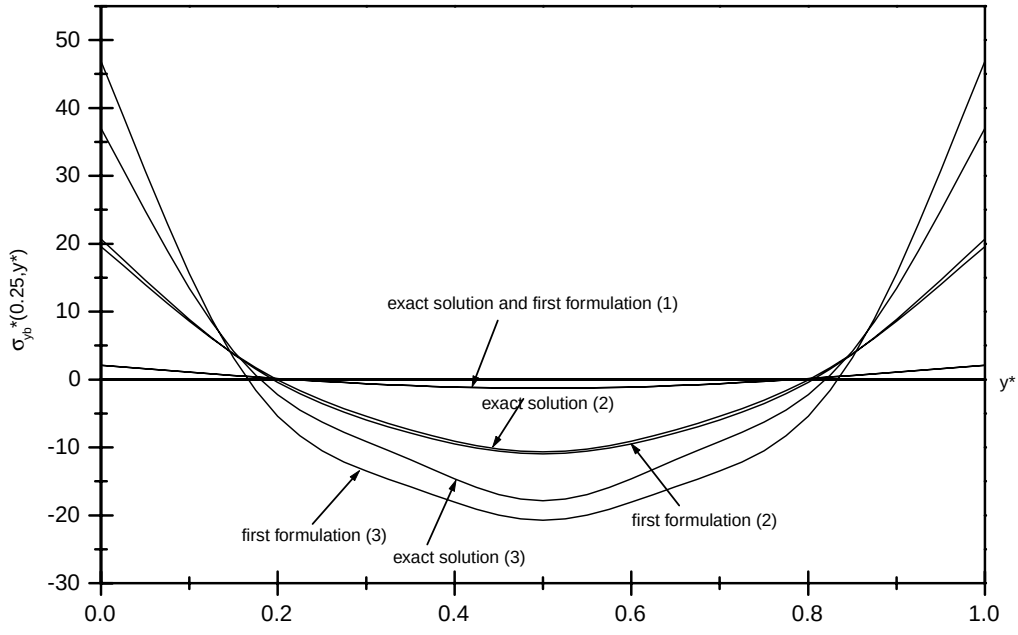

Figure 8. Non-dimensional bending stress distribution along the section $x^* = 0{\cdot}25$ of a FCRP ($\alpha = 0{\cdot}6$) obtained by the exact solution and the first formulation. First non-linear mode shape: (1) $w^*_{max} = 0{\cdot}1223$, (2) $w^*_{max} = 0{\cdot}9486$, and (3) $w^*_{max} = 1{\cdot}5093$.

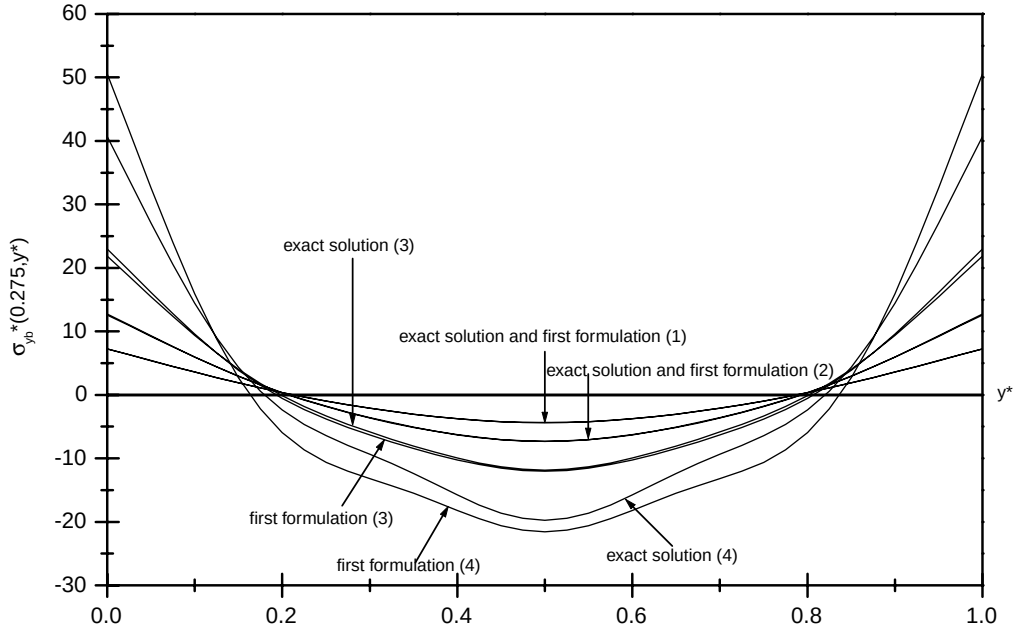

Figure 9. Non-dimensional bending stress distribution along the section $x^* = 0{\cdot}275$ of a FCRP ($\alpha = 0.6$) obtained by the exact solution and the first formulation. First non-linear mode shape: (1) $w^*_{max} = 0{\cdot}3649$, (2) $w^*_{max} = 0{\cdot}6025$, (3) $w^*_{max} = 0{\cdot}9486$, and (4) $w^*_{max} = 1{\cdot}5093$.

TABLE 6

Contribution coefficients in the BFB to the first non-linear mode shape of a FCRP, calculated via the explicit expressions obtained from application of the second formulation in the MFB, and use of the change of based rule, to obtain the corresponding basic functions contributions in the BFB ($\alpha = 0{\cdot}6$)

w^*_{max}	ω_{nl}/ω_l	a_{11}	a_{13}	a_{15}	a_{31}	a_{33}	a_{35}	a_{51}	a_{53}	a_{55}
0·122326E+00	0·100271E+01	0·500010E−01	0·287054E−03	0·412713E−04	0·168978E−02	−0·954072E−04	−0·196076E−04	0·266191E−03	−0·580177E−04	−0·146410E−04
0·244118E+00	0·101078E+01	0·100018E+00	0·645213E−03	0·112143E−03	0·364337E−02	−0·172288E−03	−0·465892E−04	0·554290E−03	−0·118704E−03	−0·284389E−04
0·364744E+00	0·102389E+01	0·150012E+00	0·114330E−02	0·241492E−03	0·610885E−02	−0·212188E−03	−0·878603E−04	0·887145E−03	−0·184160E−03	−0·406678E−04
0·483768E+00	0·104166E+01	0·200000E+00	0·184683E−02	0·457005E−03	0·931088E−02	−0·197030E−03	−0·149544E−03	0·129015E−02	−0·255620E−03	−0·508613E−04
0·600854E+00	0·106359E+01	0·250006E+00	0·281647E−02	0·784766E−03	0·134411E−01	−0·109005E−03	−0·236672E−03	0·179168E−02	−0·333089E−03	−0·588722E−04
0·715644E+00	0·108918E+01	0·300002E+00	0·410540E−02	0·124838E−02	0·186474E−01	0·692484E−04	−0·352842E−03	0·242238E−02	−0·415095E−03	−0·648981E−04
0·827977E+00	0·111801E+01	0·350002E+00	0·575997E−02	0·186923E−02	0·250393E−01	0·354757E−03	−0·500237E−03	0·321552E−02	−0·498816E−03	−0·694851E−04
0·937772E+00	0·114968E+01	0·400009E+00	0·781825E−02	0·266601E−02	0·326855E−01	0·764189E−03	−0·679533E−03	0·420560E−02	−0·580120E−03	−0·734679E−04
0·104498E+01	0·118393E+01	0·450009E+00	0·103087E−01	0·365420E−02	0·416147E−01	0·131358E−02	−0·889858E−03	0·542662E−02	−0·653754E−03	−0·778891E−04
0·114969E+01	0·122056E+01	0·500001E+00	0·132519E−01	0·484664E−02	0·518264E−01	0·201856E−02	−0·112903E−02	0·691140E−02	−0·713669E−03	−0·839045E−04
0·125207E+01	0·125947E+01	0·550013E+00	0·166622E−01	0·625424E−02	0·633016E−01	0·289467E−02	−0·139384E−02	0·869126E−02	−0·753277E−03	−0·926848E−04
0·145037E+01	0·134400E+01	0·650003E+00	0·248914E−01	0·973984E−02	0·898323E−01	0·521527E−02	−0·198157E−02	0·132355E−01	−0·743731E−03	−0·122677E−03
0·164151E+01	0·143769E+01	0·750014E+00	0·349672E−01	0·141437E−01	0·120733E+00	0·837940E−02	−0·260951E−02	0·192206E−01	−0·569722E−03	−0·174119E−03
0·182706E+01	0·154090E+01	0·850009E+00	0·467798E−01	0·194628E−01	0·155433E+00	0·124693E−01	−0·322626E−02	0·267269E−01	−0·179349E−03	−0·248880E−03
0·200853E+01	0·165404E+01	0·950015E+00	0·601818E−01	0·256707E−01	0·193386E+00	0·175458E−01	−0·377836E−02	0·357663E−01	0·473169E−03	−0·343878E−03
0·218707E+01	0·177729E+01	0·105001E+01	0·750010E−01	0·327203E−01	0·234085E+00	0·236428E−01	−0·421342E−02	0·462892E−01	0·142586E−02	−0·451307E−03
0·297340E+01	0·245139E+01	0·150000E+01	0·154858E+00	0·731609E−01	0·441090E+00	0·635447E−01	−0·357741E−02	0·109125E+00	0·100578E−01	−0·729424E−03

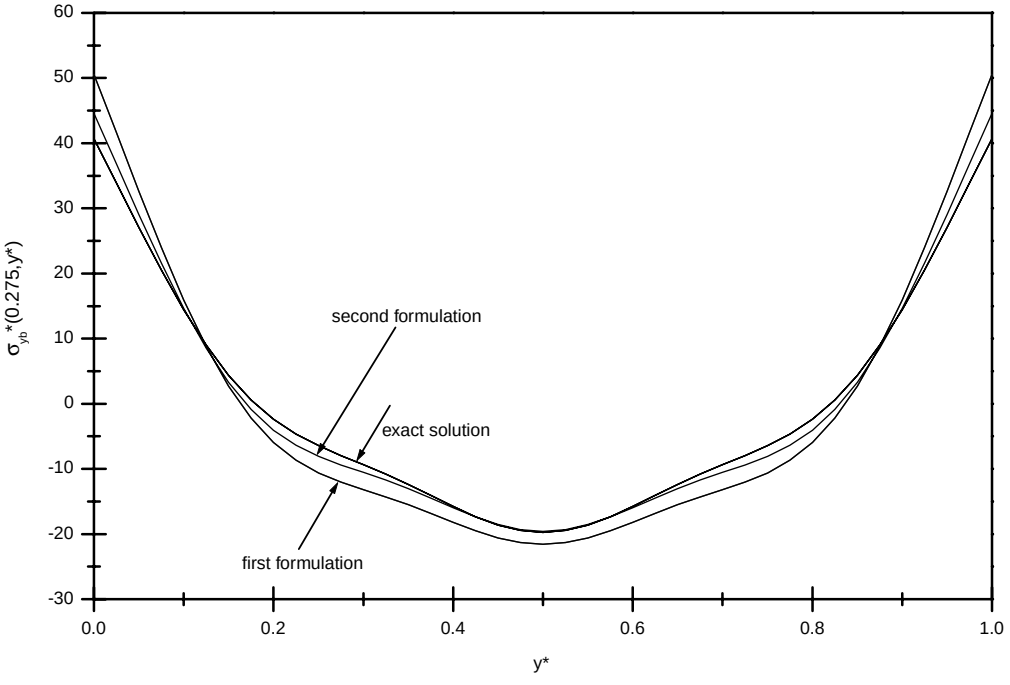

Figure 10. Non-dimensional bending stress distribution along the section $x^* = 0{\cdot}275$ of a FCRP with an aspect ratio $\alpha = 0{\cdot}6$ obtained for $w^*_{max} = 1{\cdot}5093$ by the exact solution, the first and the second formulations. First non-linear mode shape.

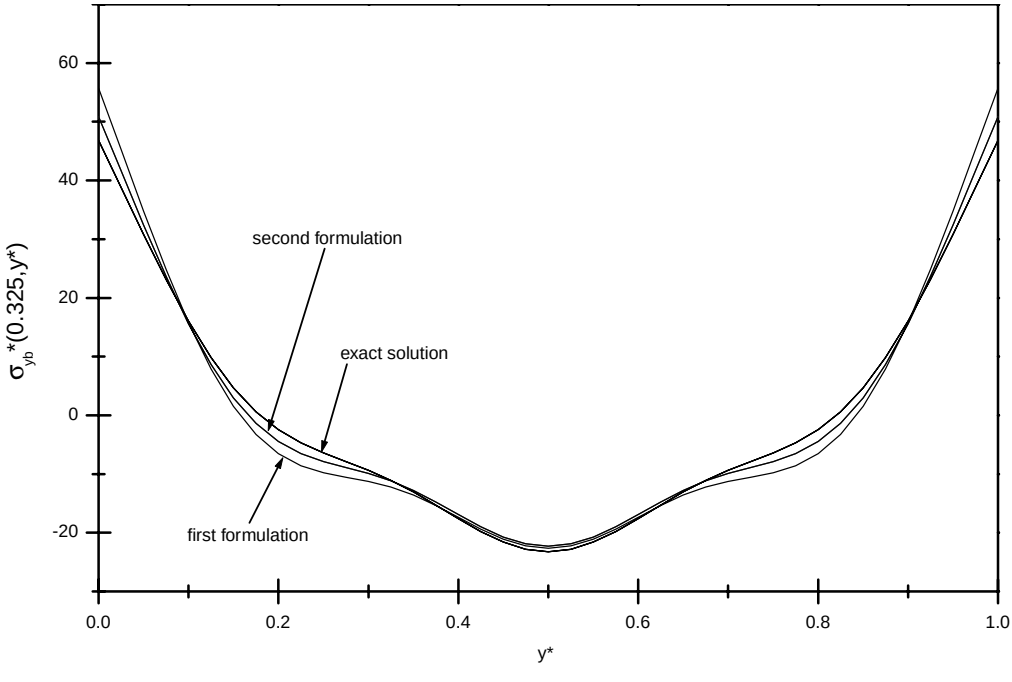

Figure 11. Non-dimensional bending stress distribution along the section $x^* = 0{\cdot}325$ of a FCRP with an aspect ratio $\alpha = 0{\cdot}6$ obtained for $w^*_{max} = 1{\cdot}5093$ by the exact solution, the first and the second formulations. First non-linear mode shape.

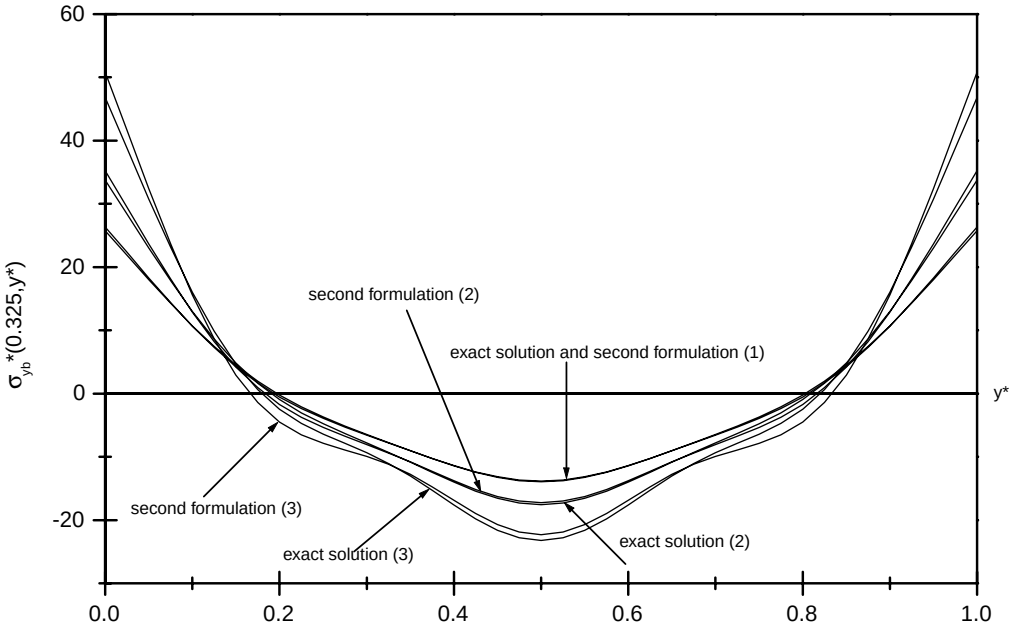

Figure 12. Non-dimensional bending stress distribution along the section $x^* = 0{\cdot}325$ of a FCRP ($\alpha = 0{\cdot}6$) obtained by the exact solution and the second formulation. First non-linear mode shape: (1) $w^*_{max} = 0{\cdot}9486$, (2) $w^*_{max} = 1{\cdot}1744$, (3) $w^*_{max} = 1{\cdot}5093$.

the non-linear algebraic system for values of the maximum non-dimensional vibration amplitude up to once the plate thickness.

4.1.3. *Effect of various truncations of the displacement series defined in equation* (58) *for the first FCRP non-linear mode shape*

In Part I of this series of papers, various possible truncations of the series expansions defining the non-linear mode shapes of the beams considered have been examined and compared with the complete solution. It has been shown that an increasing number of basic functions has to be used, corresponding to increasing ranges of vibration amplitudes, starting from use of only one function, i.e., the linear mode shape considered, corresponding to very small amplitudes for which the linear theory is still valid, and ending by the complete series. In the present paper, a similar approach has been applied to the first non-linear mode shape of FCRP. To define the truncations and the corresponding ranges, various possible truncations of series (50) have been considered and their effect on the estimated non-linear frequency and the maximum associated non-linear bending stress has been examined. It was concluded from this analysis that three interesting truncations may be adopted, involving the two, four and six functions given below, and referred to in what follows as the 2-D, 4-D, and 6-D models respectively. In Table 7, the values of the non-linear frequencies associated with the fundamental non-linear mode shape of FCRP with an aspect ratio $\alpha = 0{\cdot}6$, for various truncations of the series are summarized. It can be seen from this table, or from Figure 13, that the 2-D model, in which only the two first functions are used, leads to a good approximation of the non-linear frequency for maximum non-dimensional displacement amplitudes of vibration up to $w^*_{max} \approx 1$. In Table 8, the values of the percentage differences, obtained for various maximum vibration amplitudes, between the plate maximum

TABLE 7

Non-linear frequency parameter ω_{nl}/ω_l associated with the first non-linear mode shape of a FCRP with an aspect ratio ($\alpha = 0{\cdot}6$) obtained with various truncations of the series defined in equation (50)

w^*_{max}	9-D	2-D	4-D	6-D
0·1233E+00	0·10027E+01	0·10027E+01	0·10027E+01	0·10027E+01
0·2441E+00	0·10108E+01	0·10109E+01	0·10108E+01	0·10108E+01
0·3649E+00	0·10239E+01	0·10243E+01	0·10240E+01	0·10240E+01
0·4844E+00	0·10417E+01	0·10429E+01	0·10418E+01	0·10417E+01
0·6025E+00	0·10636E+01	0·10662E+01	0·10638E+01	0·10637E+01
0·7191E+00	0·10893E+01	0·10941E+01	0·10896E+01	0·10893E+01
0·8344E+00	0·11181E+01	0·11261E+01	0·11187E+01	0·11183E+01
0·9486E+00	0·11499E+01	0·11620E+01	0·11511E+01	0·11505E+01
0·10619E+01	0·11840E+01	0·12014E+01	0·11871E+01	0·11864E+01
0·11744E+01	0·12203E+01	0·12439E+01	0·12276E+01	0·12268E+01
0·12864E+01	0·12584E+01	0·12893E+01	0·12741E+01	0·12733E+01

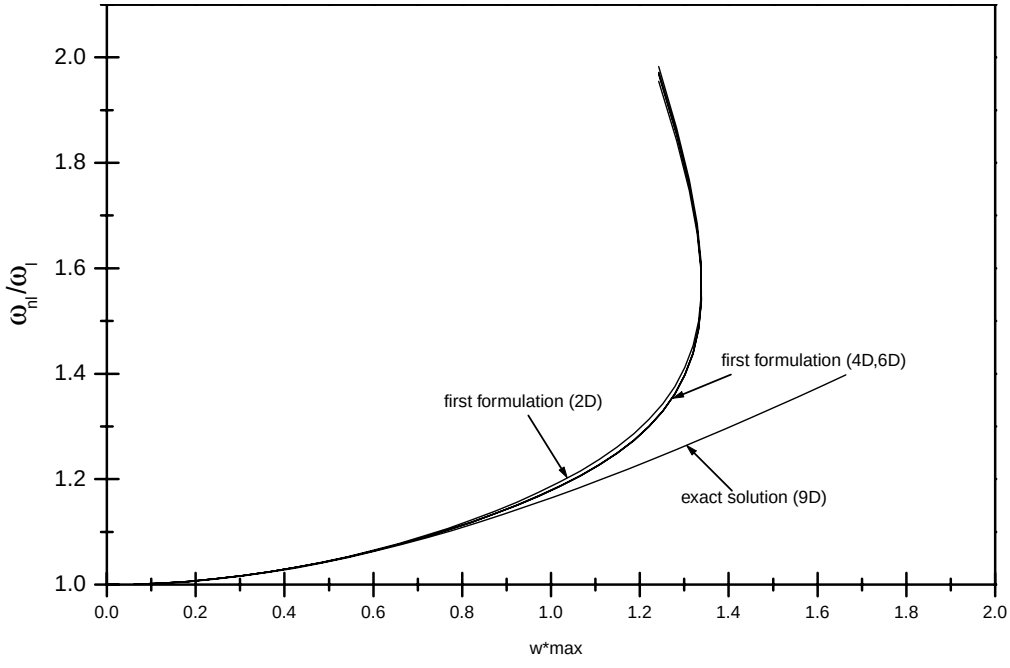

Figure 13. Non-linear frequency parameter of a FCRP with an aspect ratio ($\alpha = 0{\cdot}6$) obtained with various truncations of the series defined in equations (51–53).

non-dimensional bending stress calculated via the iterative solution of the non-linear algebraic system, and that calculated via the first formulation using various truncations are listed, which leads to the following conclusions.

2-*D model*: A comparison of the percentage difference corresponding to different models permits one to conclude that the fundamental non-linear mode shape can be approximated with a percentage error on the associated maximum non-linear bending stress which does

TABLE 8

Percentage error r between the values of the maximum bending stress associated with the first non-linear mode shape of a FCRP with an aspect ratio ($\alpha = 0{\cdot}6$) *obtained by the complete series defined in equation* (50), *and various truncations of the series.* $r = |Max(\sigma_{yb*nD} - \sigma_{yb*ex})/Max(\sigma_{yb*ex})|$

w^*_{max}	2-D	4-D	6-D	9-D
0·1223	0·61%	0·094%	0·027%	0·0070%
0·2441	4·78%	0·78%	0·24%	0·11%
0·3649	15·67%	2·80%	0·99%	0·53%
0·4844	35·8%	7·06%	2·77%	1·98%
0·6025	67·01%	14·73%	6·33%	5·52%

not exceed 1%, using the 2-D model, for amplitudes up to 0.13 times the plate thickness. So, the fundamental non-linear mode shape may be approximated, for this range of amplitudes of vibration, by the following expression; involving only two-plate modal functions, corresponding to the two first SSFCRP mode shapes:

$$w^*_{nl1}(x^*, y^*, \bar{a}_1) = \bar{a}_1 \phi^*_1(x^*, y^*) + \frac{913{\cdot}69\bar{a}_1^3}{((670{\cdot}47 + 1461{\cdot}21\bar{a}_1^2) - 3242{\cdot}59)} \phi^*_2(x^*, y^*). \quad (51)$$

4-*D model*: For amplitudes of vibration up to 0·25 times the plate thickness, the 4-D model may be used with a percentage error on the associated non-linear bending stress of less than 1%. This leads to the following expression, involving four basic functions, corresponding to the four SSFCRP mode shapes ϕ^*_1, ϕ^*_2, ϕ^*_4 and ϕ^*_7:

$$\begin{aligned} w^*_{nl1}(x^*, y^*, \bar{a}_1) = {} & \bar{a}_1 \phi^*_1(x^*, y^*) + \frac{913{\cdot}69\bar{a}_1^3}{((670{\cdot}47 + 1461{\cdot}21\bar{a}_1^2) - 3242{\cdot}59)} \phi^*_2(x^*, y^*) \\ & + \frac{1446{\cdot}57\bar{a}_1^3}{((670{\cdot}47 + 1461{\cdot}21\bar{a}_1^2) - 15483{\cdot}28)} \phi^*_4(x^*, y^*) \\ & + \frac{-3448{\cdot}09\bar{a}_1^3}{((670{\cdot}47 + 1461{\cdot}21\bar{a}_1^2) - 91294{\cdot}62)} \phi^*_7(x^*, y^*). \end{aligned} \quad (52)$$

6-*D model*: For amplitudes of vibration up to 0·36 the plate thickness, the 6-D model may be used with a percentage error on the associated non-linear bending stress of less than 1%. This leads to the following expression, involving six basic functions, corresponding to the first six SSFCRP mode shapes ϕ^*_1, ϕ^*_2, ϕ^*_3, ϕ^*_4, ϕ^*_7 and ϕ^*_8:

$$\begin{aligned} w^*_{nl1}(x^*, y^*, \bar{a}_1) = {} & \bar{a}_1 \phi^*_1(x^*, y^*) + \frac{913{\cdot}69\bar{a}_1^3}{((670{\cdot}47 + 1461{\cdot}21\bar{a}_1^2) - 3242{\cdot}59)} \phi^*_2(x^*, y^*) \\ & + \frac{267{\cdot}04\bar{a}_1^3}{((670{\cdot}47 + 1461{\cdot}21\bar{a}_1^2) - 14261{\cdot}23)} \phi^*_3(x^*, y^*) \\ & + \frac{1446{\cdot}57\bar{a}_1^3}{((670{\cdot}47 + 1461{\cdot}21\bar{a}_1^2) - 15483{\cdot}28)} \phi^*_4(x^*, y^*) \end{aligned}$$

$$+\frac{-3448{\cdot}09\bar{a}_1^3}{((670{\cdot}47+1461{\cdot}21\bar{a}_1^2)-91294{\cdot}62)}\phi_7^*(x^*,y^*)$$

$$+\frac{1746{\cdot}84\bar{a}_1^3}{((670{\cdot}47+1461{\cdot}21\bar{a}_1^2)-109581{\cdot}94)}\phi_8^*(x^*,y^*). \tag{53}$$

For higher vibration amplitudes, up to 0·6 times the plate thickness, the complete series (50) has to be used, with a percentage error which does not exceed 0·06% for the non-linear frequency and 5·6% for the non-linear bending stress estimates.

4.2. EXPLICIT ANALYTICAL EXPRESSION FOR THE SECOND FCRP NON-LINEAR MODE SHAPE CORRESPONDING TO $\alpha = 0{\cdot}6$

Replacing in equation (45) the FCRP modal parameters corresponding to the second non-linear mode shape of FCRP with an aspect ratio $\alpha = 0{\cdot}6$ by their numerical values given in Appendix B, leads to the following explicit expression of the second non-linear mode shape of this plate, involving nine terms:

$$w'^*_{nl2}(x^*,y^*,\bar{a}'_1)=\bar{a}'_1\phi_1^{*\prime}(x^*,y^*)+\frac{-2649{,}97\bar{a}_1'^3}{((1389{\cdot}59+3885{\cdot}43\bar{a}_1'^2)-7128{\cdot}56)}\phi_2^{*\prime}(x^*,y^*)$$

$$+\frac{2793{,}05\bar{a}_1'^3}{((1389{\cdot}59+3885{\cdot}43\bar{a}_1'^2)-18243{\cdot}57)}\phi_3^{*\prime}(x^*,y^*)$$

$$+\frac{367{,}82\bar{a}_1'^3}{((1389{\cdot}59+3885{\cdot}43\bar{a}_1'^2)-26145{\cdot}86)}\phi_4^{*\prime}(x^*,y^*)$$

$$+\frac{923{,}40\bar{a}_1'^3}{((1389{\cdot}59+3885{\cdot}43\bar{a}_1'^2)-31947{\cdot}77)}\phi_5^{*\prime}(x^*,y^*)$$

$$+\frac{-2274{,}66\bar{a}_1'^3}{((1389{\cdot}59+3885{\cdot}43\bar{a}_1'^2)-63949{\cdot}00)}\phi_6^{*\prime}(x^*,y^*)$$

$$+\frac{-2805{,}20\bar{a}_1'^3}{((1389{\cdot}59+3885{\cdot}43\bar{a}_1'^2)-97874{\cdot}30)}\phi_7^{*\prime}(x^*,y^*)$$

$$+\frac{486{,}19\bar{a}_1'^3}{((1389{\cdot}59+3885{\cdot}43\bar{a}_1'^2)-126845{\cdot}71)}\phi_8^{*\prime}(x^*,y^*)$$

$$+\frac{-1968{,}84\bar{a}_1'^3}{((1389{\cdot}59+3885{\cdot}43\bar{a}_1'^2)-184259{\cdot}95)}\phi_9^{*\prime}(x^*,y^*), \tag{54}$$

in which x^* and y^* are the non-dimensional geometrical co-ordinates defined in equation (16), which vary in the interval [0, 1], and $\phi_1^{*\prime}, \phi_2^{*\prime}, \ldots, \phi_9^{*\prime}$ are the first nine ASFCRP linear mode shapes, whose components in the BFB′ are given in Appendix B.

In Table 9, numerical results for function contributions to the second non-linear mode shape of FCRP having an aspect ratio $\alpha = 0{\cdot}6$, calculated via the first formulation are summarized. Comparison of this table with Table 3, taken from reference [19], in which the function contributions have been obtained by solving iteratively the non-linear algebraic

TABLE 9

Contribution coefficients in the BFB to the second non-linear mode shape of a FCRP, calculated via the explicit expressions obtained from application of the first formulation in the MFB, and use of the change of based rule, to obtain the corresponding basic functions contributions in the BFB ($\alpha = 0{\cdot}6$)

w^*_{max}	ω_{nl}/ω_l	a_{21}	a_{23}	a_{25}	a_{41}	a_{43}	a_{45}	a_{61}	a_{63}	a_{65}
0·117006E+00	0·100348E+01	0·500E−01	0·95324E−03	0·139176E−03	0·13296E−02	−0·119060E−03	−0·301803E−04	0·269613E−03	−0·643464E−04	−0·244848E−04
0·233207E+00	0·101380E+01	0·100E+00	0·20302E−02	0·301564E−03	0·30113E−02	−0·233694E−03	−0·575076E−04	0·529871E−03	−0·100469E−03	−0·554611E−04
0·347598E+00	0·103050E+01	0·150E+00	0·33547E−02	0·510184E−03	0·54067E−02	−0·338730E−03	−0·789825E−04	0·771091E−03	−0·799988E−04	−0·993891E−04
0·459441E+00	0·105304E+01	0·200E+00	0·50570E−02	0·788801E−03	0·89103E−02	−0·428078E−03	−0·914375E−04	0·984355E−03	0·2575459E−04	−0·162899E−03
0·567620E+00	0·108079E+01	0·250E+00	0·72696E−02	0·116097E−02	0·13953E−01	−0·493425E−03	−0·912786E−04	0·116029E−02	0·2459067E−03	−0·252605E−03
0·671030E+00	0·111335E+01	0·300E+00	0·10134E−01	0·165103E−02	0·21034E−01	−0·523695E−03	−0·743809E−04	0·129006E−02	0·6103559E−03	−0·375330E−03
0·768318E+00	0·115072E+01	0·350E+00	0·13800E−01	0·228371E−02	0·30737E−01	−0·503678E−03	−0·358417E−04	0·136511E−02	0·1149791E−02	−0·538043E−03
0·857877E+00	0·119361E+01	0·400E+00	0·18432E−01	0·308447E−02	0·43769E−01	−0·412467E−03	0·303140E−04	0·137753E−02	0·1895964E−02	−0·747946E−03
0·937770E+00	0·124383E+01	0·450E+00	0·24208E−01	0·408003E−02	0·61013E−01	−0·221085E−03	0·131602E−03	0·132045E−02	0·2882353E−02	−0·101266E−02
0·100552E+01	0·130476E+01	0·500E+00	0·31330E−01	0·529835E−02	0·83597E−01	0·110899E−03	0·277693E−03	0·118851E−02	0·4144300E−02	−0·134028E−02

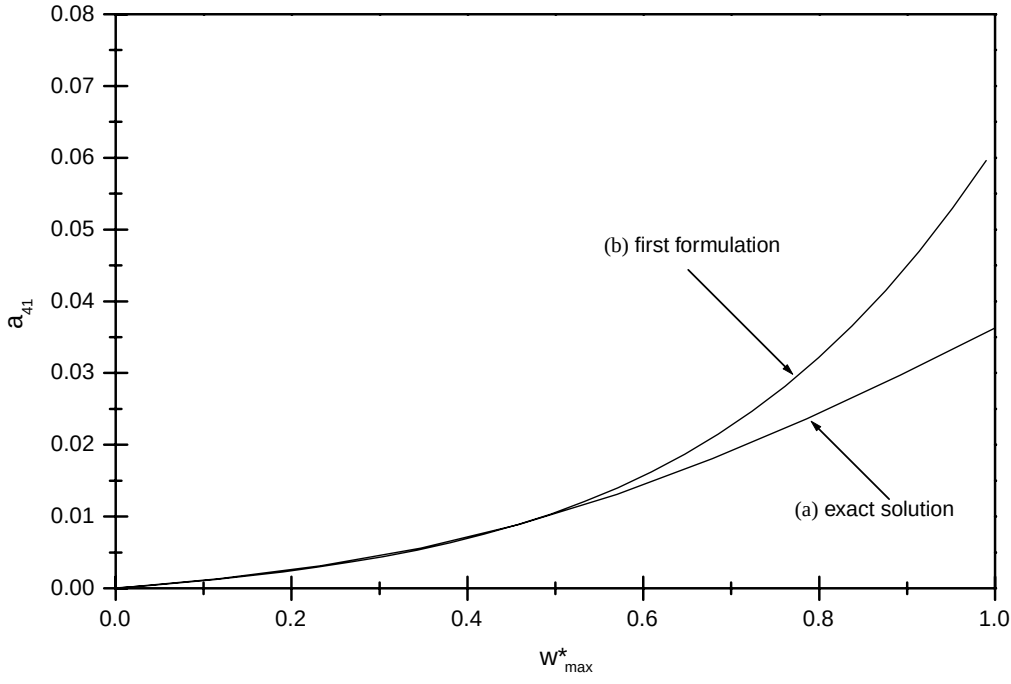

Figure 14. Comparison between the values of the contribution a_{41} to the second non-linear mode shape of a FCRP with an aspect ratio ($\alpha = 0{\cdot}6$) obtained by: (a) non-linear algebraic solution, and (b) first formulation.

system leads to the same conclusion as that given above for the fundamental FCRP non-linear mode shape: the higher basic function contributions to the second non-linear FCRP mode shape, or the first ASFCRP non-linear mode shape, obtained from the explicit expressions based on the first formulation, applied in the MFB′, are very close to those calculated via the solution of the non-linear algebraic system, for maximum non-dimensional plate amplitudes of vibration up to 0·5 times the plate thickness, obtained at point $(x^*, y^*) = (0{\cdot}29,\ 0{\cdot}50)$.[†] This is illustrated in Figures 14–17, in which the basic function contributions of the most significantly contributing functions, i.e., a_{41}, a_{23}, a_{61} and a_{25}, expressed in the BFB′, obtained from application of the first formulation in the MFB′, are plotted versus the maximum non-dimensional plate vibration amplitude w^*_{max}, obtained at point $(x^*, y^*) = (0{\cdot}29,\ 0{\cdot}50)$, and compared with the exact iterative solution of the non-linear algebraic system (23). To have an accurate conclusion concerning the limit of validity of the first explicit solution for the FCRP second non-linear mode shape, i.e., equation (54), in engineering applications, a criterion based on the effect of the differences appearing in the estimated contributions to physical quantities, such as the associated non-linear frequency and bending stress distribution has been adopted. It was found, as may be seen in Figure 18, that for amplitudes of vibration up to 0·6 times the plate thickness, the error induced by the first formulation does not exceed 0·36% for the non-linear frequency. For the bending stress distribution obtained from the contributions calculated via the first formulation, it may be seen from Figure 19 that it remains very close to that based on the contributions calculated via iterative solution of the non-linear algebraic system for values of the maximum non-dimensional vibration amplitude up to $w^*_{max} \approx 0{\cdot}6$.

[†]As has been noticed in reference [19], the point at which the maximum vibration amplitude associated with the second non-linear mode shape of a FCRP moves toward the clamps when the amplitude of vibration increases.

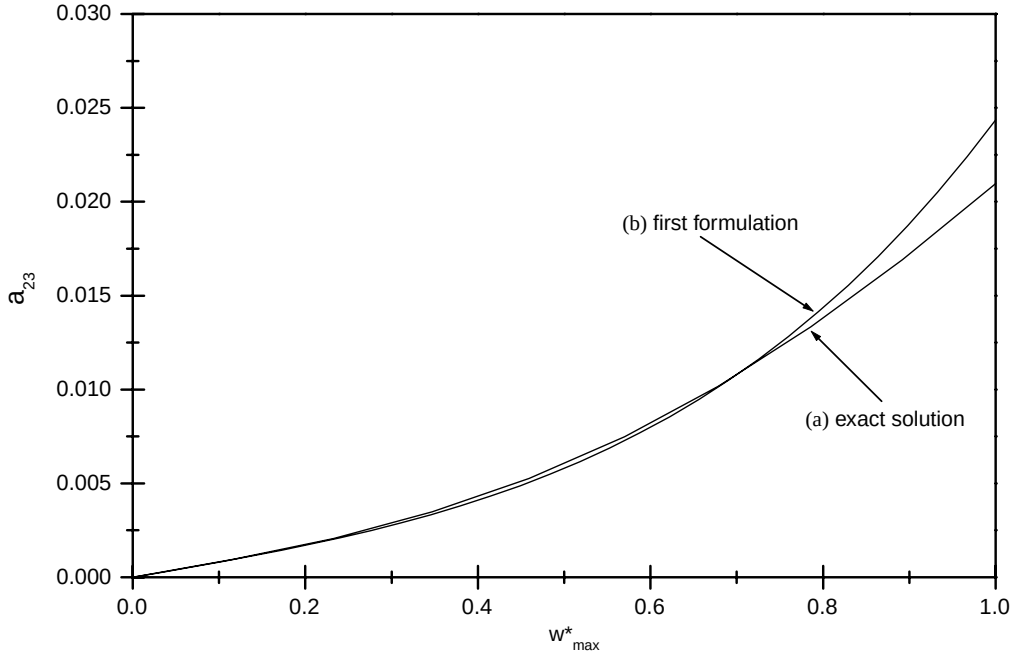

Figure 15. Comparison between the values of the contribution a_{23} to the second non-linear mode shape of a FCRP with an aspect ratio ($\alpha = 0{\cdot}6$) obtained by: (a) non-linear algebraic solution, and (b) first formulation.

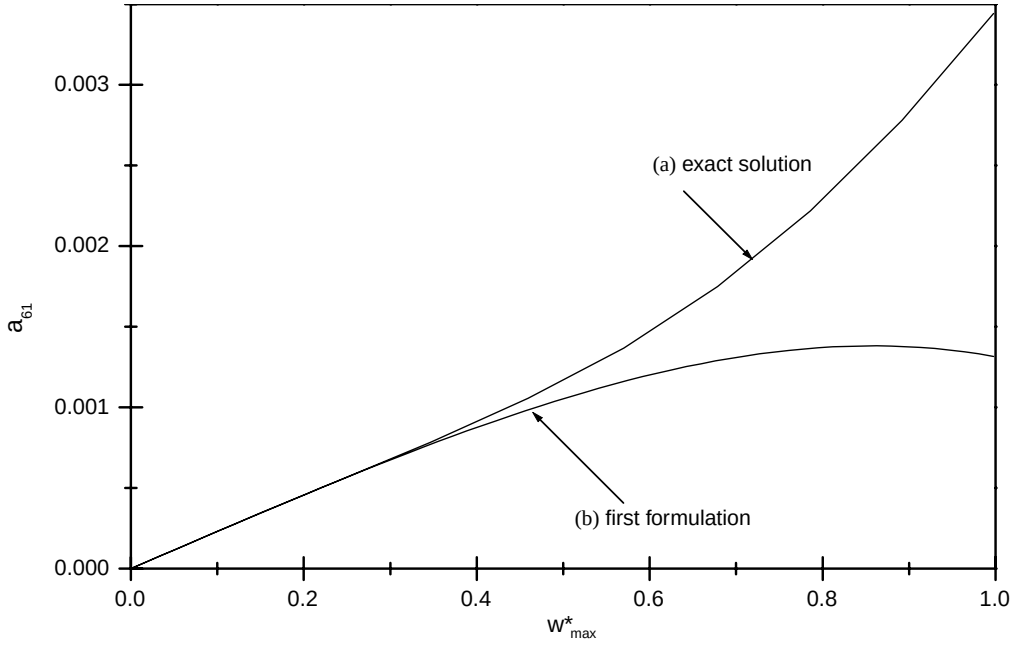

Figure 16. Comparison between the values of the contribution a_{61} to the second non-linear mode shape of a FCRP with an aspect ratio ($\alpha = 0{\cdot}6$) obtained by: (a) non-linear algebraic solution, and (b) first formulation.

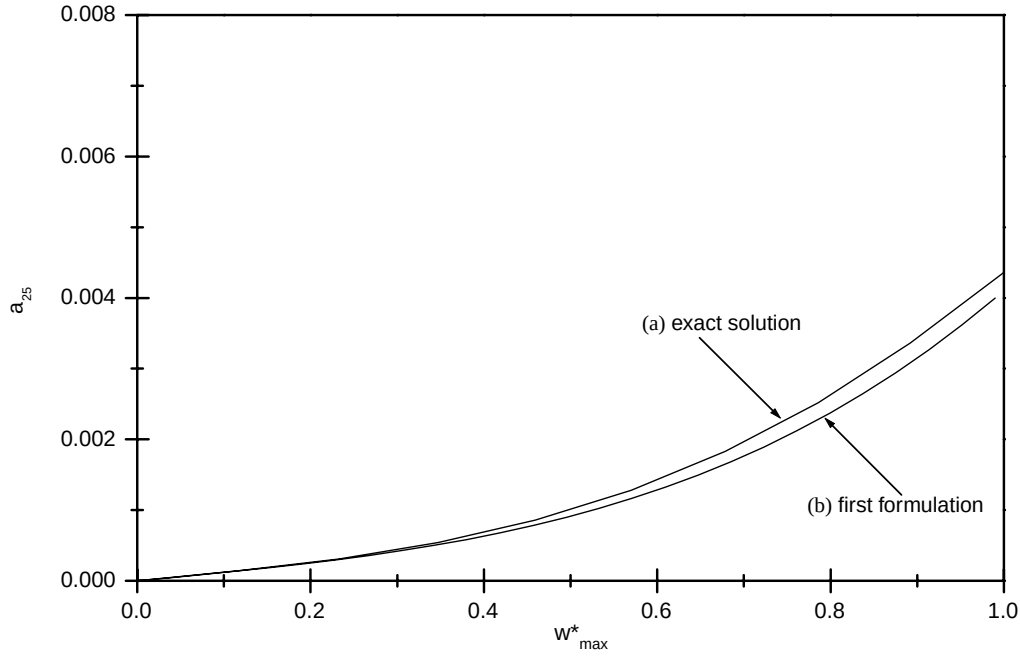

Figure 17. Comparison between the values of the contribution a_{25} to the second non-linear mode shape of a FCRP with an aspect ratio ($\alpha = 0{\cdot}6$) obtained by: (a) non-linear algebraic solution, and (b) first formulation.

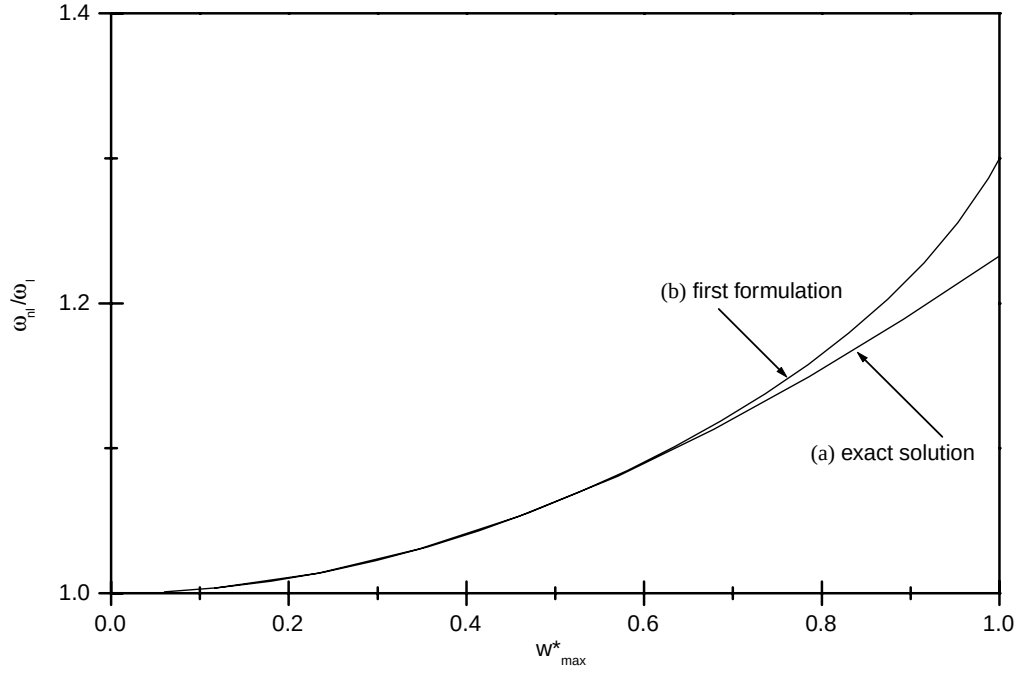

Figure 18. Comparison between frequency parameter ω_{nl}/ω_l associated with the second non-linear FCRP mode shape ($\alpha = 0{\cdot}6$), obtained by: (a) non-linear algebraic equations, and (b) first formulation.

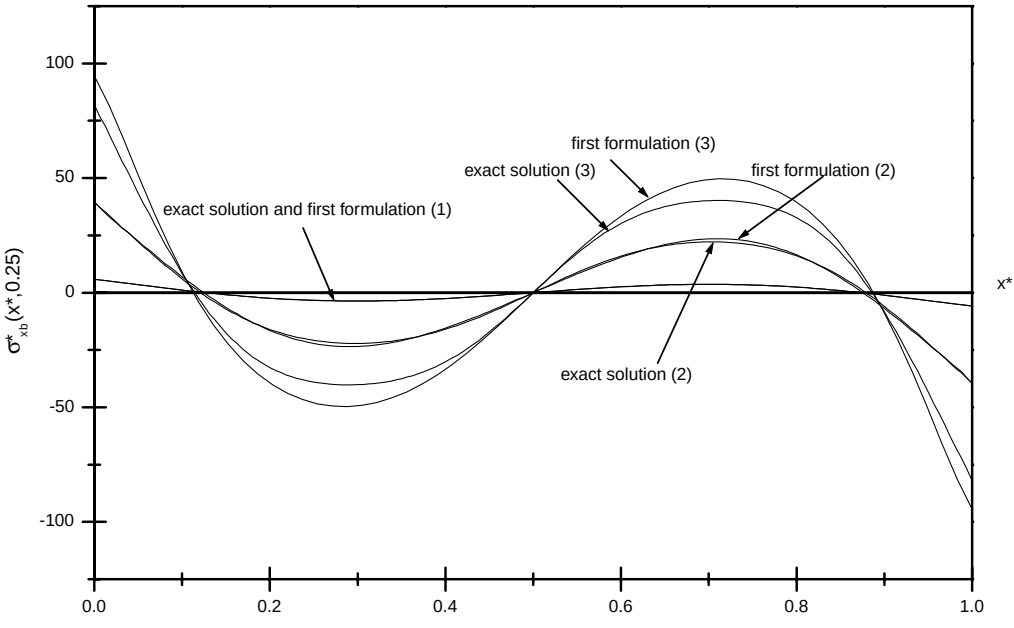

Figure 19. Non-dimensional bending stress distribution along the section $y^* = 0{\cdot}25$ of a FCRP with an aspect ratio ($\alpha = 0{\cdot}6$) obtained by the exact solution and the first formulation. Second non-linear mode shape: (1) $w^*_{max} = 0{\cdot}1170$, (2) $w^*_{max} = 0{\cdot}6787$, and (3) $w^*_{max} = 1{\cdot}2072$.

5. GENERAL CONCLUSION

In the free vibration case, explicit analytical expressions for the higher mode contribution coefficients to the first SSFCRP non-linear mode shape, and to the first ASFCRP non-linear mode shape, have been obtained. These expressions practically coincide with the numerical solution of the non-linear algebraic system previously developed for amplitudes up to 0·6 times the plate thickness for the first SSFCRP non-linear mode shape, and up to 0·5 times the plate thickness for the first ASFCRP non-linear mode shape. For displacement amplitudes between 0·6 times the plate thickness and the plate thickness, associated with the first non-linear SSFCRP mode shape, an improved complementary formulation is presented, which leads to the exact numerical solution, via the solution of a linear system of eight equations and eight unknowns, for each value of the amplitude of vibration. These two formulations make it very easy to obtain the non-linear mode shapes and resonance frequencies of FCRP for finite amplitudes of vibration.

Approximate expressions have been given for the first FCRP non-linear mode shape, corresponding to different intervals of vibration amplitudes. These expressions have been obtained by various truncations of the series expansion defining the first FCRP non-linear mode shape, based on the first formulation. It was shown that an increasing number of modal functions has to be used, corresponding to increasingly sized intervals of vibration amplitude, starting from use of only one function, i.e., the first linear mode shape, corresponding to very small amplitudes for which the linear theory is still valid, and ending by the complete series, involving nine functions.

Numerical results obtained from application of the two models to the first and second mode shapes of FCRP with an aspect ratio $\alpha = 0{\cdot}6$ have been given. Data concerning the higher FCRP non-linear mode shapes, other aspect ratios, are expected to be obtained easily by extending the present theory. This will be presented later.

A similar approach will also be applied to the forced periodic response case, enabling explicit determination of the non-linear multi-mode steady state periodic forced response of FCRP.

REFERENCES

1. R. G. WHITE 1978 *Composites* **9**, 251–258. A comparison of some statistical properties of the response of aluminium alloy and CFRP plates to acoustic excitations.
2. H. WOLFE 1995 *Ph.D. Thesis, University of Southampton.* An experimental investigation of non-linear beams and plates exited to high levels of dynamic response.
3. C. MEI and K. R. WENTZ 1982 *American Institute of Aeronautics and Astronautics Journal* **20**, 1450–1458. Large-amplitude random response of angle-ply laminated composite plates.
4. R. G. WHITE 1990 *Composite Structures* **16**, 171–192. Developments in the acoustic fatigue design process for composite aircraft structures.
5. L. AZRAR 1999 *Ph.D. Thesis, University Mohammed V of Rabat*. Semi-analytical and asymptotic-numerical methods for non-linear vibrations. Applications to large amplitude vibrations of beams and plates.
6. R. BENAMAR 1990 *Ph.D. Thesis, University of Southampton.* Non-linear dynamic behaviour of fully clamped beams and rectangular isotropic and laminated plates.
7. A. W. LEISSA 1969 *NASA-SP* **160**, 58–67. Vibration of plates.
8. A. W. LEISSA 1973 *Journal of Sound and Vibration* **31**, 257–393. Free vibrations of rectangular plates.
9. C. Y. CHIA 1980 *Non-linear Analysis of Plates.* New York: McGraw-Hill.
10. A. H. NAYFEH and D. T. MOOK 1979 *Non-linear Oscillations.* New York: John Wiley.
11. H. N. CHU and G. HERMANN 1956 *Journal of Applied Mechanics* **23**, 532–540. Influence of large amplitudes on free flexural vibrations of rectangular elastic plates.
12. L. W. REHFIELD 1973 *International Journal of Solids and Structures*, **9**, 581–590. Non-linear free vibrations of elastic structures.
13. R. BENAMAR, M. M. K. BENNOUNA and R. G. WHITE 1991 *Journal of Sound and Vibration* **149**, 179–195. The effects of large vibration amplitudes on the mode shapes and natural frequencies of thin elastic structures. Part I: simply supported and clamped–clamped beams.
14. H. N. CHU 1961 *Journal of the Aerospace Sciences* **28**, 602–609. Influence of large amplitudes on flexural vibrations of a thin circular cylindrical shell.
15. W. HAN and M. PETYT 1997 *Computers and Structures* **63**, 295–308. Geometrically non-linear vibration analysis of thin, rectangular plates using the hierarchical finite element method-I: the fundamental mode of isotropic plates.
16. W. HAN and M. PETYT 1997 *Computers and Structures* **63**, 309–318. Geometrically non-linear vibration analysis of thin, rectangular plates using the hierarchical finite element method-II: 1st mode of laminated plates and higher modes of isotropic and laminated plates.
17. P. RIBEIRO and M. PETYT 1999 *International Journal of Mechanical Sciences* **41**, 437–459. Non-linear vibration of plates by the hierarchical finite element and continuation methods.
18. L. AZRAR, R. BENAMAR and M. POTIER-FERRY 1998 *Journal of Sound and Vibration* **220**, 695–727. An asymptotic-numerical method for large-amplitude free vibrations of thin elastic plates.
19. M. EL KADIRI, R. BENAMAR and R. G. WHITE 1999 *Journal of Sound and Vibration* **228**, 333–358. The non-linear free vibration of fully clamped rectangular plates: second non-linear mode for various plate aspect ratios.
20. M. EL KADIRI, R. BENAMAR and R. G. WHITE 2002 *Journal of Sound and Vibration.* **249**, 263–305. Improvement of the semi-analytical method, for determining the geometrically non-linear response of thin straight structures. Part I: application to clamped–clamped and simply supported–clamped beams.
21. R. BENAMAR, M. M. K. BENNOUNA and R. G. WHITE 1991 *Journal of Sound and Vibration* **164**, 399–424. The effects of large vibration amplitudes on the mode shapes and natural frequencies of thin elastic structures. Part II: fully clamped rectangular isotropic plates.
22. L. AZRAR, R. BENAMAR and R. G. WHITE 1999 *Journal of Sound and Vibration* **224**, 377–395. A semi-analytical approach to the non-linear dynamic response. Problem of S–S and C–C beams at large vibration amplitudes. Part I: general theory and application to the single mode approach to free and forced vibration analysis.

23. L. AZRAR, R. BENAMAR and R. G. WHITE 2002 *Journal of Sound and Vibration* **255**, 1–41. A semi-analytical approach to the non-linear dynamic response problem of beams at large vibration amplitudes. Part II: multimode approach to the forced vibration analysis.
24. R. BENAMAR, M. M. K. BENNOUNA and R. G. WHITE 1994 *Journal of Sound and Vibration* **175**, 377–395. The effects of large vibration amplitudes on the mode shapes and natural frequencies of thin elastic structures. Part III: fully clamped rectangular isotropic plates—measurements of the mode shape amplitude dependence and the spatial distribution of harmonic distortion.
25. B. HARRAS, R. BENAMAR and R. G. WHITE 2002 *Journal of Sound and Vibration* **252**, 281–315. Experimental and theoretical investigation of the linear and non-linear dynamic behaviour of a Glare 3 hybrid composite panel.
26. F. MOUSSAOUI, R. BENAMAR and R. G. WHITE 2000 *Journal of Sound and Vibration* **232**, 917–943. The effect of large vibration amplitudes on the mode shapes and natural frequencies of thin elastic shells. Part I: coupled transverse-circumferential mode shapes of isotropic circular cylindrical shells of infinite length.
27. B. HARRAS, R. BENAMAR and R. G. WHITE 2002 *Journal of Sound and Vibration* **251**, 579–619. Geometrically non-linear free vibration of fully clamped symmetrically laminated rectangular composite plates.
28. S. TIMOSHENKO and S. WOINOWSKY-KRIEGER 1959. *Theory of Plates and Shells*, p. 345. New York: McGraw-Hill; second edition.
29. R. G. WHITE 1971 *Journal of Sound and Vibration* **16**, 255–267. Effects of non-linearity due to large deflections in the resonance testing of structures.
30. D. YOUNG 1950 *Journal of Applied Mechanics*, **December**, 448–453. Vibration of the rectangular plates by the Ritz method.

APPENDIX A: NUMERICAL DETAILS OF FCRP ANALYSIS

The chosen basic functions w_{ij}^* have been obtained as a product of the linear clamped–clamped beam functions in the x and y directions:

$$w_{ij}^*(x^*, y^*) = f_i^*(x^*) \times f_j^*(y^*) \tag{A1}$$

with

$$f_i^*(x^*) = \frac{(\mathrm{ch}(v_i x^*) - \cos(v_i x^*))}{(\mathrm{ch}\, v_i - \cos v_i)} - \frac{(\mathrm{sh}(v_i x^*) - \sin(v_i x^*))}{(\mathrm{sh}\, v_i - \sin v_i)}, \tag{A2}$$

where v_i, for $i = 1,2, \ldots$ are the eigenvalue parameters for a clamped–clamped beam.

The values of the parameters v_i have been computed by solving numerically the transcendental equation $\mathrm{ch}\, v_i \cos v_i = 1$ using Newton's method and are given in Table A1. The functions f_i^* have been normalized in such a manner that

$$m_{ij}^* = \int_0^1 f_i^*(x^*) f_j^*(x^*)\, \mathrm{d}x^* = \delta_{ij}. \tag{A3}$$

TABLE A1

Symmetric (a) *and antisymmetric* (b) *eigenvalue parameters for a clamped–clamped beam*

	(a)		(b)
1	4·73004075	2	7·85320462
3	10·99560784	4	14·13716549
5	17·27875966	6	20·42035225
7	23·56194490	8	26·70353756
9	29·84513021	10	32·98672286
11	36·12831552	12	39·26990817

APPENDIX B: LINEAR AND NON-LINEAR MODAL PARAMETERS FOR THE FCRP FIRST AND SECOND NON-LINEAR MODE SHAPES CALCULATION. ASPECT RATIO $\alpha = 0{\cdot}6$

(1) *Values of non-linear FCRP modal parameters*: $\bar{b}^*_{i111}$ *for the first non-linear FCRP mode shape and* $\bar{b}'^*_{i11}$ *for the second non-linear FCRP mode shape.*

$$\bar{b}^*_{1111} = 1461{\cdot}20989046, \qquad \bar{b}'^*_{1111} = 3885{\cdot}42971345,$$

$$\bar{b}^*_{2111} = 609{\cdot}12803852, \qquad \bar{b}'^*_{2111} = -1766{\cdot}64404353,$$

$$\bar{b}^*_{3111} = 178{\cdot}02385498, \qquad \bar{b}'^*_{3111} = 1862{\cdot}03316985,$$

$$\bar{b}^*_{4111} = 964{\cdot}37854234, \qquad \bar{b}'^*_{4111} = 245{\cdot}21328319,$$

$$\bar{b}^*_{5111} = -47{\cdot}90243557, \qquad \bar{b}'^*_{5111} = 615{\cdot}60263925,$$

$$\bar{b}^*_{6111} = 202{\cdot}51822941, \qquad \bar{b}'^*_{6111} = -1516{\cdot}43987900,$$

$$\bar{b}^*_{7111} = -2298{\cdot}72645034, \qquad \bar{b}'^*_{7111} = -1870{\cdot}13312816,$$

$$\bar{b}^*_{8111} = 1164{\cdot}55719747, \qquad \bar{b}'^*_{8111} = 324{\cdot}12779714,$$

$$\bar{b}^*_{9111} = -198{\cdot}97939619, \qquad \bar{b}'^*_{9111} = -1312{\cdot}56075265.$$

(2) *Rigidity matrix for the first non-linear mode shape of FCRP with an aspect ratio* $\alpha = 0{\cdot}6$ *expressed in the BFB*:

$$[k^*_{ij}] = \begin{bmatrix}
674{\cdot}4143 & -86{\cdot}1874 & -67{\cdot}4566 & -86{\cdot}1860 & 68{\cdot}1604 & 53{\cdot}3234 & -67{\cdot}4299 & 53{\cdot}3234 & 41{\cdot}7161 \\
-86{\cdot}1874 & 15558{\cdot}7014 & -215{\cdot}8281 & 68{\cdot}1604 & -692{\cdot}9366 & 170{\cdot}3977 & 53{\cdot}3234 & -542{\cdot}1252 & 133{\cdot}3061 \\
-67{\cdot}4565 & -215{\cdot}8281 & 91540{\cdot}9905 & 53{\cdot}3234 & 170{\cdot}3977 & -1850{\cdot}0956 & 41{\cdot}7161 & 133{\cdot}3061 & -1447{\cdot}5055 \\
-86{\cdot}1860 & 68{\cdot}1604 & 53{\cdot}3234 & 3271{\cdot}1858 & -692{\cdot}9313 & -542{\cdot}1285 & -215{\cdot}5138 & 170{\cdot}3977 & 133{\cdot}3061 \\
68{\cdot}1604 & -692{\cdot}9366 & 170{\cdot}3977 & -692{\cdot}9313 & 23556{\cdot}5089 & -1732{\cdot}6789 & 170{\cdot}3977 & -1732{\cdot}5269 & 425{\cdot}9869 \\
53{\cdot}3234 & 170{\cdot}3977 & -1850{\cdot}0956 & -542{\cdot}1285 & -1732{\cdot}6789 & 109839{\cdot}1056 & 133{\cdot}3061 & 425{\cdot}9869 & -4626{\cdot}2467 \\
-67{\cdot}4299 & 53{\cdot}3234 & 41{\cdot}7161 & -215{\cdot}5138 & 170{\cdot}3977 & 133{\cdot}3061 & 14391{\cdot}9895 & -1850{\cdot}0548 & -1447{\cdot}3859 \\
53{\cdot}3234 & -542{\cdot}1252 & 133{\cdot}3061 & 170{\cdot}3977 & -1732{\cdot}5269 & 425{\cdot}9869 & -1850{\cdot}0548 & 44977{\cdot}6201 & -4625{\cdot}5414 \\
41{\cdot}7161 & 133{\cdot}3061 & -1447{\cdot}5055 & 133{\cdot}3061 & 425{\cdot}9869 & -4626{\cdot}2467 & -1447{\cdot}3859 & -4625{\cdot}5414 & 150903{\cdot}9226
\end{bmatrix}$$

(3) *First nine SSFCRP linear mode shapes*:

$$\phi_1^* = \begin{bmatrix} 0{\cdot}9994 \\ 0{\cdot}0055 \\ 0{\cdot}0007 \\ 0{\cdot}0329 \\ -0{\cdot}0020 \\ -0{\cdot}0004 \\ 0{\cdot}0052 \\ -0{\cdot}0012 \\ -0{\cdot}0003 \end{bmatrix}, \quad \phi_2^* = \begin{bmatrix} 0{\cdot}0329 \\ 0{\cdot}0041 \\ 0{\cdot}0006 \\ -0{\cdot}9987 \\ -0{\cdot}0342 \\ -0{\cdot}0056 \\ -0{\cdot}0181 \\ 0{\cdot}0020 \\ 0{\cdot}0007 \end{bmatrix}, \quad \phi_3^* = \begin{bmatrix} 0{\cdot}0045 \\ 0{\cdot}0217 \\ 0{\cdot}0005 \\ 0{\cdot}0178 \\ 0{\cdot}0106 \\ 0{\cdot}0013 \\ -0{\cdot}9976 \\ -0{\cdot}0611 \\ -0{\cdot}0127 \end{bmatrix}, \quad \phi_4^* = \begin{bmatrix} 0{\cdot}0054 \\ -0{\cdot}9954 \\ -0{\cdot}0026 \\ -0{\cdot}0005 \\ -0{\cdot}0903 \\ 0{\cdot}0002 \\ -0{\cdot}0211 \\ -0{\cdot}0249 \\ 0{\cdot}0002 \end{bmatrix}, \quad \phi_5^* = \begin{bmatrix} 0{\cdot}0037 \\ -0{\cdot}0920 \\ -0{\cdot}0024 \\ -0{\cdot}0343 \\ 0{\cdot}9919 \\ 0{\cdot}0195 \\ 0{\cdot}0032 \\ 0{\cdot}0779 \\ 0{\cdot}0004 \end{bmatrix},$$

$$\phi_6^* = \begin{bmatrix} 0{\cdot}0012 \\ -0{\cdot}0164 \\ -0{\cdot}0015 \\ 0{\cdot}0059 \\ -0{\cdot}0791 \\ -0{\cdot}0054 \\ -0{\cdot}0625 \\ 0{\cdot}9938 \\ 0{\cdot}0427 \end{bmatrix}, \quad \phi_7^* = \begin{bmatrix} -0{\cdot}0007 \\ -0{\cdot}0025 \\ 0{\cdot}9937 \\ -0{\cdot}0000 \\ -0{\cdot}0000 \\ 0{\cdot}1073 \\ 0{\cdot}0001 \\ 0{\cdot}0006 \\ 0{\cdot}0325 \end{bmatrix}, \quad \phi_8^* = \begin{bmatrix} 0{\cdot}0006 \\ 0{\cdot}0023 \\ -0{\cdot}1102 \\ -0{\cdot}0048 \\ -0{\cdot}0196 \\ 0{\cdot}9879 \\ -0{\cdot}0003 \\ -0{\cdot}0009 \\ 0{\cdot}1070 \end{bmatrix}, \quad \phi_9^* = \begin{bmatrix} 0{\cdot}0002 \\ 0{\cdot}0010 \\ -0{\cdot}0206 \\ 0{\cdot}0012 \\ 0{\cdot}0053 \\ -0{\cdot}1097 \\ -0{\cdot}0100 \\ -0{\cdot}0435 \\ 0{\cdot}9927 \end{bmatrix}.$$

The above vector components are given in the $BFB = \{w_{11}^*, w_{13}^*, w_{15}^*, w_{31}^*, w_{33}^*, w_{35}^*, w_{51}^*, w_{53}^*, w_{55}^*\}$.

(4) *Diagonal rigidity matrix for the first non-linear mode shape of FCRP with an aspect ratio* $\alpha = 0.6$ *expressed in MFB*:

$$[\bar{k}_{ij}^*] = \begin{bmatrix} 670{\cdot}4738 & & & & & & & & \\ & 3242{\cdot}5882 & & & & & & & \\ & & 14261{\cdot}2275 & & & & & & \\ & & & 15483{\cdot}2756 & & & & & \\ & & & & 23475{\cdot}3007 & & & & \\ & & & & & 45040{\cdot}8070 & & & \\ & & & & & & 91294{\cdot}6209 & & \\ & & & & & & & 109581{\cdot}9417 & \\ & & & & & & & & 151664{\cdot}2037 \end{bmatrix}$$

(5) *First nine ASFCRP linear mode shapes*:

$$\phi_1'^* = \begin{bmatrix} 0{\cdot}9994 \\ 0{\cdot}0186 \\ 0{\cdot}0027 \\ 0{\cdot}0254 \\ -0{\cdot}0024 \\ -0{\cdot}0006 \\ 0{\cdot}0054 \\ -0{\cdot}0014 \\ -0{\cdot}0005 \end{bmatrix}, \quad \phi_2'^* = \begin{bmatrix} -0{\cdot}0252 \\ -0{\cdot}0066 \\ -0{\cdot}0010 \\ 0{\cdot}9983 \\ 0{\cdot}0489 \\ 0{\cdot}0090 \\ 0{\cdot}0133 \\ -0{\cdot}0016 \\ -0{\cdot}0007 \end{bmatrix}, \quad \phi_3'^* = \begin{bmatrix} 0{\cdot}0183 \\ -0{\cdot}9951 \\ -0{\cdot}0095 \\ -0{\cdot}0018 \\ -0{\cdot}0928 \\ 0{\cdot}0000 \\ 0{\cdot}0071 \\ -0{\cdot}0276 \\ 0{\cdot}0007 \end{bmatrix}, \quad \phi_4'^* = \begin{bmatrix} -0{\cdot}0051 \\ 0{\cdot}0064 \\ -0{\cdot}0007 \\ -0{\cdot}0126 \\ -0{\cdot}0135 \\ -0{\cdot}0017 \\ 0{\cdot}9971 \\ 0{\cdot}0718 \\ 0{\cdot}0161 \end{bmatrix}$$

$$\phi_5'^* = \begin{bmatrix} 0{\cdot}0055 \\ -0{\cdot}0941 \\ -0{\cdot}0043 \\ -0{\cdot}0493 \\ 0{\cdot}9916 \\ 0{\cdot}0307 \\ 0{\cdot}0086 \\ 0{\cdot}0666 \\ 0{\cdot}0008 \end{bmatrix}, \quad \phi_6'^* = \begin{bmatrix} 0{\cdot}0019 \\ -0{\cdot}0216 \\ -0{\cdot}0036 \\ 0{\cdot}0058 \\ -0{\cdot}0677 \\ -0{\cdot}0066 \\ -0{\cdot}0731 \\ 0{\cdot}9933 \\ 0{\cdot}0536 \end{bmatrix}, \quad \phi_7'^* = \begin{bmatrix} -0{\cdot}0024 \\ -0{\cdot}0095 \\ 0{\cdot}9919 \\ -0{\cdot}0001 \\ -0{\cdot}0005 \\ 0{\cdot}1198 \\ 0{\cdot}0001 \\ 0{\cdot}0019 \\ 0{\cdot}0421 \end{bmatrix}, \quad \phi_8'^* = \begin{bmatrix} 0{\cdot}0010 \\ 0{\cdot}0042 \\ -0{\cdot}1233 \\ -0{\cdot}0074 \\ -0{\cdot}0311 \\ 0{\cdot}9870 \\ -0{\cdot}0004 \\ -0{\cdot}0012 \\ 0{\cdot}0980 \end{bmatrix}, \quad \phi_9'^* = \begin{bmatrix} -0{\cdot}0004 \\ -0{\cdot}0019 \\ 0{\cdot}0297 \\ -0{\cdot}0014 \\ -0{\cdot}0063 \\ 0{\cdot}1022 \\ 0{\cdot}0122 \\ 0{\cdot}0548 \\ -0{\cdot}9927 \end{bmatrix}.$$

The above vector components are given in the $BFB' = \{w_{21}^*, w_{23}^*, w_{25}^*, w_{41}^*, w_{43}^*, w_{45}^*, w_{61}^*, w_{63}^*, w_{65}^*\}$.

(6) *Diagonal rigidity matrix for the second non-linear mode shape of FCRP with an aspect ratio* $\alpha = 0{\cdot}6$ *expressed in MFB'*:

$$[\bar{k}_{ij}'^*] = \begin{bmatrix} 1389{\cdot}5893 & & & & & & & & \\ & 7128{\cdot}5637 & & & & & & & \\ & & 18243{\cdot}567 & & & & & & \\ & & & 26145{\cdot}864 & & & & & \\ & & & & 31947{\cdot}769 & & & & \\ & & & & & 63949{\cdot}002 & & & \\ & & & & & & 97874{\cdot}302 & & \\ & & & & & & & 126845{\cdot}71 & \\ & & & & & & & & 184259{\cdot}95 \end{bmatrix}.$$

APPENDIX C: PROOF OF EQUATION (34)

In the BFB, the transverse displacement function $w^*(x^*, y^*)$ has been written in the form of a finite series:

$$w^*(x^*, y^*) = a_i w_i^*(x^*, y^*) = \{\mathbf{A}\}^{\mathrm{T}}\{\mathbf{w}^*\} \tag{C1}$$

with $\{\mathbf{A}\}^{\mathrm{T}} = [a_1 a_2 \ldots a_n]$, and $\{\mathbf{w}^*\}^{\mathrm{T}} = [w_1^* w_2^* \ldots w_n^*]$, in which $w_i^*(x^*, y^*)$ is the ith element of the BFB defined in Appendix A.

In the MFB, $w^*(x^*, y^*)$ has been written as

$$w^*(x^*, y^*) = \bar{a}_i \phi_i^*(x^*, y^*) = \{\bar{\mathbf{A}}\}^{\mathrm{T}} \{\boldsymbol{\phi}^*\} \tag{C2}$$

with $\{\bar{\mathbf{A}}\}^{\mathrm{T}} = [\bar{a}_1 \bar{a}_2 \dots \bar{a}_n]$ and $\{\phi^*\}^{\mathrm{T}} = [\phi_1^* \phi_2^* \dots \phi_n^*]$, where $\phi_r^*(x^*, y^*)$ is the rth linear mode shape of the FCRP considered, given by

$$\phi_r^*(x^*, y^*) = \phi_{rs} w_s^*(x^*, y^*). \tag{C3}$$

This defines the transition matrix from the BFB to the MFB as

$$[\boldsymbol{\phi}] = [\boldsymbol{\phi}_{rs}] \tag{C4}$$

so that equation (C3) can be written in a matrix form as

$$\{\boldsymbol{\phi}^*\} = [\boldsymbol{\phi}_{rs}] \{\mathbf{w}^*\}. \tag{C5}$$

Now, combining (C1) and (C2), one obtains

$$\{\bar{\mathbf{A}}\}^{\mathrm{T}} \{\boldsymbol{\phi}^*\} = \{\mathbf{A}\}^{\mathrm{T}} \{\mathbf{w}^*\}. \tag{C6}$$

Replacing from (C5) $\{\boldsymbol{\phi}^*\}$ by $[\boldsymbol{\phi}]\{\mathbf{w}^*\}$ leads to

$$\{\bar{\mathbf{A}}\}^{\mathrm{T}} [\boldsymbol{\phi}] \{\mathbf{w}^*\} = \{\mathbf{A}\}^{\mathrm{T}} \{\mathbf{w}^*\}. \tag{C7}$$

Therefore, we have, after identification and transposition:

$$\{\mathbf{A}\} = [\boldsymbol{\phi}]^{\mathrm{T}} \{\bar{\mathbf{A}}\} \tag{C8}$$

which may be written in tensorial form as

$$a_s = \phi_{rs} \bar{a}_r. \tag{C9}$$

Combining equations (5) and (14), one obtains for the maximum bending strain energy, over a period of vibration:

$$V_b = a_i a_j k_{ij}^* = \phi_{ri} \bar{a}_r \phi_{sj} \bar{a}_s k_{ij}^* = \bar{a}_r \bar{a}_s \bar{k}_{rs}^*, \tag{C10}$$

which shows that

$$\bar{k}_{rs}^* = \phi_{ri} \phi_{sj} k_{ij}^*, \tag{C11}$$

in the same manner, one obtains from consideration of the kinetic energy T:

$$\bar{m}_{rs}^* = \phi_{ri} \phi_{sj} m_{ij}^*. \tag{C12}$$

Similarly, we can write for the non-linear strain energy V_a:

$$V_a = a_i a_j a_k a_l b^*_{ijkl} = \phi_{ri}\bar{a}_r\phi_{sj}\bar{a}_s\phi_{uk}\bar{a}_u\phi_{vl}\bar{a}_v b^*_{ijkl} = \bar{a}_r\bar{a}_s\bar{a}_u\bar{a}_v\bar{b}^*_{rsuv}, \tag{C13}$$

which gives the expression for

$$\bar{b}^*_{rsuv} = \phi_{ri}\phi_{sj}\phi_{uk}\phi_{vl}b^*_{ijkl} \tag{C14}$$

APPENDIX D: EXPRESSIONS OF THE NON-DIMENSIONAL BENDING STRESSES

The maximum bending strains ε_{xb} and ε_{yb} obtained for $z = H/2$ are given by

$$\varepsilon_{xb} = \frac{H}{2}\left(\frac{\partial^2 w}{\partial x^2}\right), \quad \varepsilon_{yb} = \frac{H}{2}\left(\frac{\partial^2 w}{\partial y^2}\right). \tag{D1, 2}$$

Using the classical thin-plate assumption of plane stress and Hooke's law, the corresponding bending stresses can be obtained as

$$\sigma_{xb} = \frac{EH}{2(1-v^2)}\left(\left(\frac{\partial^2 w}{\partial x^2}\right) + v\left(\frac{\partial^2 w}{\partial y^2}\right)\right), \tag{D3}$$

$$\sigma_{yb} = \frac{EH}{2(1-v^2)}\left(\left(\frac{\partial^2 w}{\partial y^2}\right) + v\left(\frac{\partial^2 w}{\partial x^2}\right)\right). \tag{D4}$$

In terms of the non-dimensional parameters defined in reference [3], the non-dimensional bending stresses σ^*_{xb} and σ^*_{yb} can be defined by

$$\sigma^*_{xb} = \alpha^2\left(\frac{\partial^2 w^*}{\partial x^{*2}}\right) + v\left(\frac{\partial^2 w^*}{\partial y^{*2}}\right), \tag{D5}$$

$$\sigma^*_{yb} = \left(\frac{\partial^2 w^*}{\partial y^{*2}}\right) + v\alpha^2\left(\frac{\partial^2 w^*}{\partial y^{*2}}\right). \tag{D6}$$

The relationships between dimensional and non-dimensional bending stresses are

$$\sigma = \frac{EH^2}{2(1-v^2)}\sigma^*. \tag{D7}$$

APPENDIX E: NOMENCLATURE

General notation

V_b, V_a and V	bending, axial and total strain energy respectively
T	kinetic energy
E	Young's modulus
v	the Poisson ratio
D	bending stiffness, $D = EH^3/12(1-v^2)$
ρ	mass density per unit volume of the plate
a, b	length, width of the plate
α	the plate aspect ratio $\alpha = b/a$
S, S^*	dimensional and non-dimensional surfaces $[0,a]\times[0,b]$ and $[0,1]\times[0,1]$ respectively
H	thickness of the plate

FCRP	fully clamped rectangular plate, or fully clamped rectangular plates, depending on the context.
(x, y)	point co-ordinates.
$W(x, y, t)$	transverse displacement at point (x, y) on the plate
U and V	in-plane displacements in the x and y directions respectively
*	the star exponent indicates non-dimensional parameters
$w_{ij}(x, y)$	basic function obtained as product of the ith clamped–clamped beam function in the x direction, with the jth clamped–clamped beam function in the y direction.
q_i	generalized co-ordinate $q_i(t) = a_i \sin(\omega t)$
HFEM	hierarchical finite element method

First FCRP non-linear mode shape

ω,ω^*	frequency and non-dimensional frequency parameter respectively (first non-linear mode shape)
$\{\mathbf{A}\}$	column matrix of basic function contributions to the first non-linear mode shape, corresponding to the BFB
$\{\bar{\mathbf{A}}\}$	column matrix of modal function contributions to the first non-linear mode shape, corresponding to the MFB
k_{ij}, m_{ij}, and b_{ijkl}	general term of the rigidity tensor, the mass tensor and the non-linearity tensor respectively
$[\mathbf{K}]$, $[\mathbf{M}]$,$[\mathbf{B}]$	rigidity, mass and non-linearity matrix, respectively, for the first non-linear mode shape
$[\bar{\mathbf{K}}]$,$[\bar{\mathbf{M}}]$,$[\bar{\mathbf{B}}]$	rigidity, mass and non-linearity matrix, expressed in modal functions basis, respectively, for the first non-linear mode shape
$\bar{k}^*_{ij}$, $\bar{m}^*_{ij}$, and, $\bar{b}^*_{ijkl}$	general term of the non-dimensional rigidity tensor, mass tensor and non-linearity tensor, respectively, in the MFB for the first non-linear mode shape
SS mode	a mode shape of the FCRP considered which is symmetric in both the x and y directions
ϕ^*_i	the ith linear SS mode shape of the FCRP
BFB	beam functions basis for the first SS mode. This basis is made of FCRP functions which are obtained as products of symmetric clamped–clamped beam functions, in both the x and y directions. $BFB = \{w^*_{11}, w^*_{13}, w^*_{15}, w^*_{31}, w^*_{33}, w^*_{35}, w^*_{51}, w^*_{53}, w^*_{55}\}$
MFB	modal functions basis for the first SS mode, made of the first nine SSFCRF linear mode shapes. The components of the modal functions in the BFB are given in Appendix B $MFB = \{\phi^*_1, \phi^*_2, \phi^*_3, \phi^*_4, \phi^*_5, \phi^*_6, \phi^*_7, \phi^*_8, \phi^*_9\}$
$[\bar{a}_{11}\bar{\varepsilon}_{31} \ldots \bar{\varepsilon}_{55}]^{\mathrm{T}}$	column matrix of the modal function contribution coefficients to the first non-linear SSFCRP mode shape
$w^*_{nl1}(x^*, y^*, \bar{a}_1)$	the first SSFCRP non-linear mode shape for a given assigned value $\bar{a}_1$ of the first SS modal function contribution

Second FCRP non-linear mode shape

ω', $\omega^{*\prime}$	frequency and non-dimensional frequency parameter respectively (second non-linear mode shape)
$\{\mathbf{A}'\}$	column matrix of basic function contributions to the second non-linear mode shape, corresponding to the BFB′
$\{\bar{\mathbf{A}}'\}$	column matrix of modal function contributions to the second non-linear mode shape, corresponding to the MFB′
$[\mathbf{K}']$,$[\mathbf{M}']$,$[\mathbf{B}']$	rigidity, mass and non-linearity matrix, respectively, for the second non-linear mode shape
$[\bar{\mathbf{K}}']$,$[\bar{\mathbf{M}}']$,$[\bar{\mathbf{B}}']$	rigidity, mass and non-linearity matrix, expressed in the modal functions basis, respectively, for the second non-linear mode shape
$\bar{k}^{*\prime}_{ij}$, $\bar{m}^{*\prime}_{ij}$, and, $\bar{b}^{*\prime}_{ijkl}$	general terms of the non-dimensional rigidity tensor, mass tensor and non-linearity tensor, respectively, in the MFB′ for the second non-linear mode shape
AS mode	a mode shape of the FCRP considered which is antisymmetric in the x direction and symmetric in the y direction
$\phi^{*\prime}_i$	the ith linear AS mode shape of the FCRP

BFB' beam functions basis for the first AS mode. This basis is made of FCRP functions which are obtained as products of antisymmetric clamped–clamped beam functions, in the x direction, with symmetric clamped–clamped beam functions in the y direction.
$BFB' = \{w^*_{21}, w^*_{23}, w^*_{25}, w^*_{41}, w^*_{43}, w^*_{45}, w^*_{61}, w^*_{63}, w^*_{65}\}$

MFB' modal functions basis for the first AS mode, made of the first nine ASFCRP linear mode shapes. The components of the modal functions in the BFB' are given in Appendix B
$MFB' = \{\phi^{*\prime}_1, \phi^{*\prime}_2, \phi^{*\prime}_3, \phi^{*\prime}_4, \phi^{*\prime}_5, \phi^{*\prime}_6, \phi^{*\prime}_7, \phi^{*\prime}_8, \phi^{*\prime}_9\}$

$[\bar{a}_{21}\bar{\varepsilon}_{23} \ldots \bar{\varepsilon}_{65}]^{\mathrm{T}}$ column matrix of the modal function contribution coefficients to the second non-linear ASFCRP mode shape

$w^{*\prime}_{nl2}(x^*, y^*, \bar{a}_1)$ the first ASFCRP non-linear mode shape for a given assigned value $\bar{a}_1$ of the first AS modal function contribution